Far field model for time reversal and application to selective focusing on small dielectric inhomogeneities

Corinna Burkard, Aurelia Minut, Karim Ramdani

Far field model for time reversal and application to selective focusing on small dielectric inhomogeneities

Corinna BURKARD[*] [†] [‡] Aurelia MINUT[§] Karim RAMDANI[*†‡]

Abstract

Based on the time-harmonic far field model for small dielectric inclusions in 3D, we study the so-called DORT method (DORT is the French acronym for “Diagonalization of the Time Reversal Operator”). The main observation is to relate the eigenfunctions of the time-reversal operator to the location of small scattering inclusions. For non penetrable sound-soft acoustic scatterers, this observation has been rigorously proved for 2 and 3 dimensions by Hazard and Ramdani in [20] for small scatterers. In this work, we consider the case of small dielectric inclusions with far field measurements. The main difference with the acoustic case is related to the magnetic permeability and the related polarization tensors. We show that in the regime $kd \to \infty$ (k denotes here the wavenumber and d the minimal distance between the scatterers), each inhomogeneity gives rise to -at most- 4 distinct eigenvalues (one due to the electric contrast and three to the magnetic one) while each corresponding eigenfunction generates an incident wave focusing selectively on one of the scatterers. The method has connections to the MUSIC algorithm known in Signal Processing and the Factorization Method of Kirsch.

Keywords

Time-reversal, scattering, small inhomogeneities, far field operator, wave focusing.

Mathematics Subject Classification

Primary: 74J20, 35P25; Secondary: 78M35, 35P15, 35B40

1 Introduction

Time reversal techniques have demonstrated in the last decade their efficiency for many applications. In particular, focusing waves using time reversal mirrors (TRM) has been successfully used in medicine, submarine communications and non destructive testing (see for instance Fink et al. [17], Fink and Prada [18] or Fink [16] and references therein). In this work, we are interested in the so-called DORT method which is an experimental technique used to focus waves selectively on *small and well resolved* scatterers (i.e. when

[*]Université de Lorraine, Institut Elie Cartan de Lorraine, UMR 7502, Vandoeuvre-lès-Nancy, F-54506, France

[†]CNRS, Institut Elie Cartan de Lorraine, UMR 7502, Vandoeuvre-lès-Nancy, F-54506, France

[‡]Inria, CORIDA, Villers-lès-Nancy, F-54600, France

[§]United States Naval Academy, Mathematics Department, 572C Holloway Road, Annapolis, MD 21402-5002, USA

multiple scattering can be neglected). The case of extended (penetrable or non penetrable) obstacles is only skimmed here (see Section 3). More about inverse problems for extended scatterers can be found for instance in Arens et al. [5], Borcea et al. [7] and Hou et al. [21] in the time-harmonic case and Chen et al. [9] in the time domain. For the case of small but not necessarily distant scatterers (case where multiple scattering must be taken into account) see Devaney et al. [14]. The DORT method is in some sense related to (but different from) the MUSIC algorithm (see for instance Cheney [10], Kirsch [26] or Ammari et al. [2]) where the eigenelements of the the so-called multi-static response matrix is used to construct an indicator function of the positions of the scatterers. Let us also point out that the DORT and the MUSIC algorithm can be seen as limit cases of the Linear Sampling Method [12, 11] and Kirsch's Factorization method [23, 24, 25] for small obstacles.

Let us turn now to the description of the DORT method. Consider a homogeneous acoustic medium containing small and distant scatterers. One can generate experimentally the matrix corresponding to one cycle "Emission-Reception-Time Reversal", where the coefficient (i, j) of this matrix, is the time reversed acoustic field measured by the transducer i of the TRM when transducer j emits an impulse wave. The time reversal matrix T is then defined as the matrix corresponding to two successive cycles like the one above. It turns out the eigenelements of the time-reversal matrix carry important information on the propagation medium and on the scatterers contained in it. More precisely, according to the DORT method: 1. the number of nonzero eigenvalues of T is directly related to the number of scatterers contained in the medium, the largest eigenvalue being associated with the strongest scatterer, 2. each eigenvector generates an incident wave that selectively focuses on each scatterer.

From the mathematical point of view, this assertion has been studied in the time-harmonic case, where time reversal amounts to phase conjugation. A mathematical justification of this result has been given in Hazard and Ramdani [20] for the 3D acoustic scattering problem by small non penetrable scatterers using a far field model. In this model, the TRM was supposed to be continuous and located at infinity. For other models of TRM, we refer the reader to Ben Amar et al. [6] and Fannjiang [15]. Then, it has been extended in Pinçon and Ramdani [29] to the case of a 2D closed acoustic waveguide and in Antoine *et al.* [4] to the case of perfectly conducting electromagnetic scatterers. The case of electromagnetic time reversal has also been considered from a different point of view (more physically or numerically oriented) and with different assumptions on the TRM (near field measurements, discrete TRM) in many other references [8, 22, 28, 33]. In this work, we are interested in the case of 3D acoustic scattering by small dielectric (penetrable) inhomogeneities. Using a far field model for time reversal, we prove that for $kd \to \infty$ (k denotes here the wavenumber and d the minimal distance between the scatterers), each inhomogeneity gives rise to 4 eigenvalues (one corresponding to the dielectric contrast and three to the magnetic one). Furthermore, each corresponding eigenfunction generates an incident wave focusing selectively on one of the scatterers.

The paper is organized as follows : the mathematical setting of the problem used throughout the paper is described in Section 2. In Section 3, we give some focusing properties of the eigenfunctions of the time reversal operator in the case of extended inhomogeneities. The last three sections of the paper, constituting the core of the paper, are devoted to the case of small inhomogeneities. A mathematical justification of the DORT method is given in Sections 4 and 5, respectively in the the cases of closed and open (or finite aperture) TRM. For the latter, an additional symmetry assumption (see 5.7) on the open TRM is needed. Finally, we conclude the paper by presenting in Section 6 some numerical simulations to illustrate our theoretical results.

2 The mathematical model

We consider a three-dimensional homogeneous electromagnetic medium described by a dielectric permittivity $\varepsilon_0 > 0$ and a magnetic permeability $\mu_0 > 0$. The time dependence is supposed to be of the form $e^{-i\omega t}$ and will therefore be implicit. We assume that a local inhomogeneity is embedded in the above medium. In particular, let $\varepsilon, \mu \in L^\infty(\mathbb{R}^3)$ be strictly positive functions describing the dielectric permittivity and the magnetic permeability of the perturbed medium. We set $\mathcal{B} = \mathrm{Supp}\,(\varepsilon - \varepsilon_0) \cup \mathrm{Supp}\,(\mu - \mu_0)$ and we assume that $\mathcal{B}$ is a possibly multiply connected, smooth and bounded domain, i.e. $\mathcal{B} \subset \{|\boldsymbol{x}| < a\}$ for some $a > 0$. The outgoing unit normal to $\mathcal{B}$ is denoted ν.

We consider the scattering problem of an incident plane wave $u_I^{\boldsymbol{\alpha}}(\boldsymbol{x}) = e^{ik\boldsymbol{\alpha}\cdot\boldsymbol{x}}$ of direction $\boldsymbol{\alpha} \in S^2$, with wave number $k = \omega\sqrt{\varepsilon_0\mu_0}$ by the local inhomogeneity $\mathcal{B}$. The total field $u^{\boldsymbol{\alpha}} \in H^1_{\ell oc}(\mathbb{R}^3)$ satisfies

$$\mathrm{div}\left(\frac{1}{\mu(\boldsymbol{x})}\nabla u^{\boldsymbol{\alpha}}(\boldsymbol{x})\right) + \omega^2\varepsilon(\boldsymbol{x})u^{\boldsymbol{\alpha}}(\boldsymbol{x}) = 0 \ \text{ in } \mathbb{R}^3. \tag{2.1}$$

In order to ensure existence and uniqueness of the solution of 2.1, it has to be completed by Sommerfeld's radiation condition for the scattered field $v^{\boldsymbol{\alpha}} = u^{\boldsymbol{\alpha}} - u_I^{\boldsymbol{\alpha}}$,

$$\frac{\partial v^{\boldsymbol{\alpha}}}{\partial|\boldsymbol{x}|} - ikv^{\boldsymbol{\alpha}}(\boldsymbol{x}) = O\left(\frac{1}{|\boldsymbol{x}|^2}\right), \qquad |\boldsymbol{x}| \to \infty.$$

Denoting by $A(\boldsymbol{\alpha}, \boldsymbol{\beta})$ the scattering amplitude, the far field asymptotics of $v^{\boldsymbol{\alpha}}$ in the direction $\boldsymbol{\beta} \in S^2$ reads

$$v^{\boldsymbol{\alpha}}(\boldsymbol{\beta}|\boldsymbol{x}|) = \frac{e^{ik|\boldsymbol{x}|}}{|\boldsymbol{x}|}A(\boldsymbol{\alpha}, \boldsymbol{\beta}) + O\left(\frac{1}{|\boldsymbol{x}|^2}\right),$$

Proposition 1. *The scattering amplitude is given by the formula*

$$A(\boldsymbol{\alpha}, \boldsymbol{\beta}) = \frac{1}{4\pi}\int_{\partial\mathcal{B}}\left\{v^{\boldsymbol{\alpha}}\frac{\partial u_I^{-\beta}}{\partial\nu} - u_I^{-\beta}\frac{\partial v^{\boldsymbol{\alpha}}}{\partial\nu}\right\}\mathrm{d}s. \tag{2.2}$$

Moreover, it satisfies the reciprocity relation

$$A(\boldsymbol{\beta}, \boldsymbol{\alpha}) = A(-\boldsymbol{\alpha}, -\boldsymbol{\beta}), \qquad \forall\, \boldsymbol{\alpha}, \boldsymbol{\beta} \in S^2. \tag{2.3}$$

The proof of this result follows easily by adapting the one given in Colton and Kress [13, Theorem 8.8] for the case where μ is constant (TE case).

The far field operator $F \in \mathcal{L}(L^2(S^2))$ is defined as the integral operator with kernel $A(\cdot, \cdot)$:

$$Ff(\boldsymbol{\beta}) = \int_{S^2} A(\boldsymbol{\alpha}, \boldsymbol{\beta})\, f(\boldsymbol{\alpha})\,\mathrm{d}\boldsymbol{\alpha}.$$

By linearity of the scattering problem, note that Ff is nothing but the far field obtained after illumination of the inhomogeneity $\mathcal{B}$ by the incident Herglotz wave associated to a density $f \in L^2(S^2)$: $u_I(\boldsymbol{x}) = \int_{S^2} u_I^{\boldsymbol{\alpha}}(\boldsymbol{x}) f(\boldsymbol{\alpha})\,\mathrm{d}\boldsymbol{\alpha} = \int_{S^2} e^{ik\boldsymbol{\alpha}\cdot\boldsymbol{x}} f(\boldsymbol{\alpha})\,\mathrm{d}\boldsymbol{\alpha}$. As the kernel $A(\cdot,\cdot)$ belongs to $L^2(S^2 \times S^2)$ (in fact $A(\cdot,\cdot)$ is an infinitely differentiable function), the operator $F \in \mathcal{L}(L^2(S^2))$ is clearly compact. Moreover, since ε and μ are supposed to take real values, it is also a normal operator (this follows from a straightforward adaptation of the proof given in [13] for the TE case). Finally, the reciprocity relation 2.3 implies the following result.

Proposition 2. *The adjoint $F^* \in \mathcal{L}(L^2(S^2))$ of F is the integral operator with kernel $A^*(\boldsymbol{\alpha},\boldsymbol{\beta}) = \overline{A(-\boldsymbol{\alpha},-\boldsymbol{\beta})}$, so that: $F^*f = \overline{RF\overline{Rf}}$, where R is the symmetry operator $Rf(\boldsymbol{\alpha}) = f(-\boldsymbol{\alpha})$.*

The time reversal operator is defined as the operator corresponding to two successive cycles "Emission–Reception–Time Reversal". Recalling that reversing time amounts to a conjugation of the acoustic field when the time dependence is of the form $e^{-i\omega t}$, we see that $Tf = \overline{RF\overline{RFf}}$. The presence of the symmetry operator R in this formula indicates that a measured field in a given direction $\boldsymbol{\beta}$ is re-emitted in the opposite direction $-\boldsymbol{\beta}$. Combined to Proposition 2, the last formula yields the following result.

Theorem 3. *The time reversal operator T is the self-adjoint, compact and positive semidefinite operator given by the relation $T = F^*F = FF^*$.*

3 Global focusing

Theorem 3 implies that the far field operator F and the time reversal operator T have the same eigenfunctions (see Zaanen [35, p.442]). Furthermore, the nonzero eigenvalues of T are exactly the positive numbers $|\lambda_1|^2 \geq |\lambda_2|^2 \geq \ldots > 0$, where the complex numbers $(\lambda_p)_{p\geq 1}$ are the nonzero eigenvalues of the normal compact operator F.

Proposition 4. *Let $\lambda_p \neq 0$ be an eigenvalue of F and $f_p \in L^2(S^2)$ an eigenfunction of F associated to λ_p. Then, the incident Herglotz wave*

$$u_{I,p}(\boldsymbol{x}) = \int_{S^2} u_I^{\boldsymbol{\alpha}}(\boldsymbol{x})\, f_p(\boldsymbol{\alpha})\,\mathrm{d}\boldsymbol{\alpha}, \tag{3.1}$$

associated to f_p is given by

$$\begin{aligned} u_{I,p}(\boldsymbol{x}) = -\frac{1}{\lambda_p}\int_{\partial\mathcal{B}} \Big\{ & k j_0'(k\|\boldsymbol{x}-\boldsymbol{y}\|)\left(\nu_y \cdot \frac{\boldsymbol{x}-\boldsymbol{y}}{\|\boldsymbol{x}-\boldsymbol{y}\|}\right) v_p(\boldsymbol{y}) \\ & + j_0(k\|\boldsymbol{x}-\boldsymbol{y}\|)\,\frac{\partial v_p}{\partial \nu_{\boldsymbol{y}}}(\boldsymbol{y}) \Big\}\,\mathrm{d}s_{\boldsymbol{y}}. \end{aligned} \tag{3.2}$$

where $v_p(\boldsymbol{x}) = \displaystyle\int_{S^2} v^{\boldsymbol{\alpha}}(\boldsymbol{x})\, f_p(\boldsymbol{\alpha})\,\mathrm{d}\boldsymbol{\alpha}$ the diffracted field corresponding to the incident wave $u_{I,p}$ and $j_0(\xi) = \sin(\xi)/\xi$ is the spherical Bessel function of order 0.

Proof. Since we have by assumption $f_p(\boldsymbol{\beta}) = \lambda_p^{-1} F f_p(\boldsymbol{\beta}) = \lambda_p^{-1} \int_{S^2} A(\boldsymbol{\alpha},\boldsymbol{\beta})\, f_p(\boldsymbol{\alpha})\,\mathrm{d}\boldsymbol{\alpha}$, expression 2.2 of $A(\boldsymbol{\alpha},\boldsymbol{\beta})$ implies that

$$f_p(\boldsymbol{\beta}) = \frac{1}{4\pi\lambda_p}\int_{\partial\mathcal{B}} \left\{ \frac{\partial u_I^{-\beta}}{\partial \nu_{\boldsymbol{y}}}(\boldsymbol{y}) v_p(\boldsymbol{y}) - u_I^{-\beta}(\boldsymbol{y})\,\frac{\partial v_p}{\partial \nu_{\boldsymbol{y}}}(\boldsymbol{y}) \right\} \mathrm{d}s_{\boldsymbol{y}}.$$

The incident field generated by the eigenfunction f_p is given by

$$\begin{aligned} u_{I,p}(\boldsymbol{x}) = \frac{1}{4\pi\lambda_p}\int_{\partial\mathcal{B}} \left(\int_{S^2} \frac{\partial u_I^{-\beta}}{\partial \nu_{\boldsymbol{y}}}(\boldsymbol{y}) e^{ik\boldsymbol{\beta}\cdot\boldsymbol{x}}\, d\boldsymbol{\beta} \right) v_p(\boldsymbol{y})\,\mathrm{d}s_{\boldsymbol{y}} \\ - \frac{1}{4\pi\lambda_p}\int_{\partial\mathcal{B}} \left(\int_{S^2} e^{ik\boldsymbol{\beta}\cdot(\boldsymbol{x}-\boldsymbol{y})}\, d\boldsymbol{\beta} \right) \frac{\partial v_p}{\partial \nu_{\boldsymbol{y}}}(\boldsymbol{y})\,\mathrm{d}s_{\boldsymbol{y}}, \end{aligned}$$

Using the identity (see Abramowitz and Stegun [1, p.155])

$$\frac{1}{4\pi}\int_{S^2} e^{ik\boldsymbol{\beta}\cdot(\boldsymbol{x}-\boldsymbol{y})}\,\mathrm{d}\boldsymbol{\beta} = \frac{\sin(k\|\boldsymbol{x}-\boldsymbol{y}\|)}{k\|\boldsymbol{x}-\boldsymbol{y}\|} = j_0(k\|\boldsymbol{x}-\boldsymbol{y}\|), \tag{3.3}$$

and noting that $\dfrac{\partial u_I^{-\beta}}{\partial \nu_{\boldsymbol{y}}}(\boldsymbol{y}) = \nu_{\boldsymbol{y}} \cdot \nabla u_I^{-\beta}(\boldsymbol{y})$, we obtain

$$\frac{1}{4\pi}\int_{S^2} \nu_{\boldsymbol{y}} \cdot \nabla u_I^{-\beta}(\boldsymbol{y})\, e^{ik\boldsymbol{\beta}\cdot\boldsymbol{x}}\, d\boldsymbol{\beta} = \frac{1}{4\pi}\nu_{\boldsymbol{y}} \cdot \nabla_{\boldsymbol{y}} \int_{S^2} e^{ik\boldsymbol{\beta}\cdot(\boldsymbol{x}-\boldsymbol{y})}\,\mathrm{d}\boldsymbol{\beta} = \nu_{\boldsymbol{y}} \cdot \nabla_y \Big(j_0(k\|\boldsymbol{x}-\boldsymbol{y}\|) \Big).$$

Equation 3.2 follows then from $\nabla_{\boldsymbol{y}}\Big(j_0(k\|\boldsymbol{x}-\boldsymbol{y}\|) \Big) = -k\dfrac{\boldsymbol{x}-\boldsymbol{y}}{\|\boldsymbol{x}-\boldsymbol{y}\|} j_0'(k\|\boldsymbol{x}-\boldsymbol{y}\|)$. □

Remark 5. *Equation 3.2 shows in particular that the incident field associated to an eigenfunction f_p of F (and thus of T) focuses on the inhomogeneity, as $u_{I,p}(\boldsymbol{x})$ decreases like the inverse of the distance from $\boldsymbol{x}$ to the inhomogeneity.*

4 Selective focusing for closed time reversal mirrors

From now on, we are interested in the case of several small inclusions, and more especially in the relation between the eigenfunctions of the time-reversal operator and the location of the (asymptotically small) scatterers. We suppose that the inhomogeneity is constituted of a collection of M homogeneous small imperfections of typical size δ centered at the points $\boldsymbol{s}_p \in \mathbb{R}^3$: $\mathcal{B}^\delta = \cup_{p=1}^M (\boldsymbol{s}_p + \delta\mathcal{B}_p)$. Here, the "reference" inhomogeneities $\mathcal{B}_p \subset \mathbb{R}^3$, $p = 1, \ldots, M$ are smooth and bounded domains containing the origin. Moreover, we assume that there exist positive constants (ε_p, μ_p), $p = 1, \ldots, M$, such that

$$\begin{cases} \varepsilon^\delta(\boldsymbol{x}) = \varepsilon_0, & \mu^\delta(\boldsymbol{x}) = \mu_0, \qquad \forall\, \boldsymbol{x} \in \mathbb{R}^3 \setminus \overline{\mathcal{B}^\delta}, \\ \varepsilon^\delta(\boldsymbol{x}) = \varepsilon_p, & \mu^\delta(\boldsymbol{x}) = \mu_p, \qquad \forall\, \boldsymbol{x} \in (\boldsymbol{s}_p + \delta\mathcal{B}_p). \end{cases}$$

We also introduce the minimal distance between the inhomogeneities

$$d := \min_{1\le p<q\le M} |\boldsymbol{s}_p - \boldsymbol{s}_q| \tag{4.1}$$

Define respectively by $u^{\delta,\boldsymbol{\alpha}}$ and $v^{\delta,\boldsymbol{\alpha}}$ the total and scattered fields associated to the scattering problem of the incident plane wave $u_I^{\boldsymbol{\alpha}}(\boldsymbol{x})$ of direction $\boldsymbol{\alpha}$ by the small imperfections $\mathcal{B}^\delta$:

$$\begin{cases} \operatorname{div}\left(\dfrac{1}{\mu^\delta}\nabla u^{\delta,\boldsymbol{\alpha}}\right) + \omega^2\varepsilon^\delta u^{\delta,\boldsymbol{\alpha}} = 0 \ \text{ in } \mathbb{R}^3, \\ v^{\delta,\boldsymbol{\alpha}} := u^{\delta,\boldsymbol{\alpha}} - u_I^{\boldsymbol{\alpha}} \quad \text{is outgoing.} \end{cases} \tag{4.2}$$

Finally, let $A^\delta(\cdot,\cdot)$, F^δ and T^δ be respectively the scattering amplitude, the far field operator and the time-reversal operator associated to the above scattering problem. We first state a result due to Ammari et al. which gives an explicit representation of the asymptotic behavior of the scattering amplitude (formula (23) of [3]) .

Theorem 6. *(Ammari et al. [3, Theorem 2]) For all $p \in \{1,\dots,M\}$, we set*

$$\widetilde{\mu}_p(\boldsymbol{x}) = \begin{cases} \mu_0, & \textit{for } \boldsymbol{x} \in \mathbb{R}^3 \setminus \overline{\mathcal{B}_p}, \\ \mu_p, & \textit{for } \boldsymbol{x} \in \mathcal{B}_p. \end{cases}$$

We also introduce the following quantities measuring the electric and magnetic contrasts

$$\kappa_p^\varepsilon := \frac{\varepsilon_p}{\varepsilon_0} - 1, \qquad \kappa_p^\mu := \frac{\mu_p}{\mu_0} - 1. \tag{4.3}$$

Furthermore, let $\Phi_{p,j}$, for all $1 \le j \le 3$, be the unique solution of

$$\begin{cases} \operatorname{div}\left(\widetilde{\mu}_p(\boldsymbol{x})\nabla\Phi_{p,j}(\boldsymbol{x})\right) = 0 \qquad \text{in } \mathbb{R}^3, \\ \lim\limits_{|\boldsymbol{x}|\to\infty} \Phi_{p,j}(\boldsymbol{x}) - x_j = 0. \end{cases}$$

Let $\mathbb{M}_p = (M_{i,j}^p)_{1\le i,j\le 3}$ be the polarization tensor associated to the inhomogeneity $\mathcal{B}_p$ given by

$$M_{i,j}^p = \left(\frac{\mu_0}{\mu_p}\right)\int_{\mathcal{B}_p} \frac{\partial \Phi_{p,j}}{\partial x_i}\, d\boldsymbol{x},\ \forall 1 \le i,j \le 3.$$

Then, as $\delta \to 0$, the scattering amplitude $A^\delta(\cdot,\cdot)$ admits the asymptotics

$$A^\delta(\boldsymbol{\alpha},\boldsymbol{\beta}) = -\left(\frac{k^2}{4\pi}\right)\delta^3 A^0(\boldsymbol{\alpha},\boldsymbol{\beta}) + o(\delta^3), \tag{4.4}$$

where

$$A^0(\boldsymbol{\alpha},\boldsymbol{\beta}) = \sum_{p=1}^M e^{ik(\boldsymbol{\alpha}-\boldsymbol{\beta})\cdot \boldsymbol{s}_p}\left[\kappa_p^\mu\left(\boldsymbol{\beta}\cdot \mathbb{M}_p\,\boldsymbol{\alpha}\right) - \kappa_p^\varepsilon|\mathcal{B}_p|\right],$$

with $|\mathcal{B}_p|$ being the volume of the inclusion $\mathcal{B}_p$.

The asymptotics 4.4 holds uniformly for all $\boldsymbol{\alpha},\boldsymbol{\beta} \in S^2$ provided $\delta = o(d)$ and $\delta = o(\lambda)$, where d is defined by (4.1) and $\lambda = 2\pi/k$ denotes the wavelength.

Remark 7. *Formula (23) of [3] contains a little typo (a minus sign is missing in front of the leading term of the asymptotics) and we have corrected this in (4.4). However, this typo has no influence at all on our analysis, as we only work on the leading term $A^0(\cdot,\cdot)$ of the scattering amplitude which is defined up to a multiplicative constant.*

Remark 8. *The fact that the term $o(\delta^3)$ is uniform for all $\boldsymbol{\alpha}, \boldsymbol{\beta} \in S^2$ follows from the reciprocity relation and the last statement in [3, Theorem 1], which gives the near field asymptotics for small inhomogeneities. Indeed it is shown there that this remainder term is independent of the observation point.*

We denote by $F^0 : L^2(S^2) \longrightarrow L^2(S^2)$ the limit far field operator, namely the integral operator corresponding to A^0. From Theorem 6, the far field operator is explicitly given by

$$F^0 f(\boldsymbol{\beta}) = \sum_{p=1}^{M} \int_{S^2} e^{ik(\boldsymbol{\alpha}-\boldsymbol{\beta})\cdot \boldsymbol{s}_p} \Big\{ \kappa_p^{\mu} \left(\boldsymbol{\beta} \cdot \mathbb{M}_p \, \boldsymbol{\alpha}\right) - \kappa_p^{\varepsilon} |\mathcal{B}_p| \Big\} f(\boldsymbol{\alpha}) \, \mathrm{d}\boldsymbol{\alpha}. \tag{4.5}$$

From now on, we will study the focusing properties of the time reversal experiment using this limit far field operator. In particular, we are interested in the eigenelements of the limit time reversal operator $T^0 := (F^0)^* F^0$. As the tensor $\mathbb{M}_p$ is hermitian and positive-definite (see for instance [3] and references therein), we clearly have $\overline{A^0(\boldsymbol{\beta}, \boldsymbol{\alpha})} = A^0(\boldsymbol{\alpha}, \boldsymbol{\beta})$. Therefore, F^0 is self-adjoint and hence normal.

Remark 9. *The above result implies in particular that F^0 and T^0 have the same eigenfunctions. Moreover, the nonzero eigenvalues of T^0 are exactly the squares of the nonzero eigenvalues of the self-adjoint operator F^0 (see [35]).*

In order to study the properties of the operator F^0, let us introduce some notation. Given $p = 1, \ldots, M$, we denote by $e_p \in L^2(S^2)$ the function

$$e_p(\boldsymbol{\alpha}) := e^{-ik\boldsymbol{\alpha}\cdot \boldsymbol{s}_p}, \qquad \forall \, \boldsymbol{\alpha} \in S^2. \tag{4.6}$$

Let $\mathcal{M}_p \in \mathcal{L}(L^2(S^2))$ be the integral operator

$$\mathcal{M}_p f(\boldsymbol{\beta}) = \int_{S^2} \left(\boldsymbol{\beta} \cdot \mathbb{M}_p \, \boldsymbol{\alpha}\right) f(\boldsymbol{\alpha}) \, \mathrm{d}\boldsymbol{\alpha}, \tag{4.7}$$

Then, formula (4.5) can be rewritten in the more compact form

$$F^0 f = \sum_{p=1}^{M} \kappa_p^{\mu} \mathcal{M}_p (f \overline{e_p}) \, e_p - \kappa_p^{\varepsilon} |\mathcal{B}_p| \, (f, e_p)_{L^2(S^2)} e_p. \tag{4.8}$$

The next Lemma collects some properties of the integral operator $\mathcal{M}_p$.

Lemma 10. *The following assertions hold true.*

(i) *For all $f, g \in L^2(S^2)$, we have the identity $(\mathcal{M}_p f, g)_{L^2(S^2)} = (\mathbb{M}_p \mathbb{F}, \mathbb{G})_{\mathbb{C}^3}$, where $\mathbb{F}, \mathbb{G} \in \mathbb{C}^3$ are given by $\mathbb{F} := \int_{S^2} \boldsymbol{\alpha} f(\boldsymbol{\alpha}) \, \mathrm{d}\boldsymbol{\alpha}$ and $\mathbb{G} := \int_{S^2} \boldsymbol{\alpha} g(\boldsymbol{\alpha}) \, \mathrm{d}\boldsymbol{\alpha}$.*

(ii) *$\mathcal{M}_p \in \mathcal{L}(L^2(S^2))$ is a positive compact self-adjoint operator, and hence it is diagonalizable.*

(iii) *$\mathcal{M}_p$ is a finite rank operator : $\mathrm{Rank}\, \mathcal{M}_p \leq 3$.*

(iv) *Let $(V_{p,1}, V_{p,2}, V_{p,3})$ be an orthonormal basis of $\mathbb{C}^3$ constituted of eigenvectors of $\mathbb{M}_p$, respectively associated with the (strictly positive) eigenvalues $\xi_{p,1}, \xi_{p,2}, \xi_{p,3}$. Then, $\mathcal{M}_p$ has exactly 3 non-zero eigenvalues:*

$$\mathcal{M}_p h_{p,\ell} = \zeta_{p,\ell} h_{p,\ell}, \qquad \forall \, \ell = 1, 2, 3$$

where the eigenvalues $\zeta_{p,\ell}$ and eigenfunctions $h_{p,\ell}$ are given by

$$\zeta_{p,\ell} = \frac{4\pi}{3}\xi_{p,\ell} \qquad\qquad h_{p,\ell}(\boldsymbol{\alpha}) = \boldsymbol{\alpha} \cdot V_{p,\ell}.$$

Proof. (i) Straightforward consequence of the definition of $\mathcal{M}_p$.

(ii) The self-adjointness and positivity of $\mathcal{M}_p$ follows immediately from (i), since the polarization tensor $\mathbb{M}_p = (M^p_{i,j})_{1\le i,j\le 3}$ is a hermitian positive matrix. The compactness of the integral operator $\mathcal{M}_p$ is also clear, as it has a analytic kernel.

(iii) From expression 4.7, one clearly has $\operatorname{Ran}\mathcal{M}_p \subset \boldsymbol{\beta}\cdot\operatorname{Ran}\mathbb{M}_p$ and the result follows then from $\mathbb{M}_p$ being of rank 3.

(iv) Let us first note that $\int_{S^2}\boldsymbol{\alpha}\,\boldsymbol{\alpha}^T\,\mathrm{d}\boldsymbol{\alpha} = \frac{4\pi}{3}I$ for the identity $I \in \mathbb{R}^{3\times 3}$, which one easily verifies by using symmetry arguments or by direct calculation via spherical coordinates. Using that the vectors $V_{p,\ell}$ are eigenvectors of $\mathbb{M}_p$, we then find that

$$\mathcal{M}_p h_{p,\ell}(\boldsymbol{\beta}) = \boldsymbol{\beta}\cdot\left(\mathbb{M}_p\int_{S^2}\boldsymbol{\alpha}(\boldsymbol{\alpha}\cdot V_{p,\ell})\,\mathrm{d}\boldsymbol{\alpha}\right) = \boldsymbol{\beta}\cdot\left(\mathbb{M}_p\left[\int_{S^2}\boldsymbol{\alpha}\,\boldsymbol{\alpha}^T\,\mathrm{d}\boldsymbol{\alpha}\right]V_{p,\ell}\right) = \zeta_{p,\ell}h_{p,\ell}.$$

□

4.1 Eigenvalues and eigenfunctions of the limit far field operator

In this section we focus on the regime $kd \to \infty$, *i.e.* when the inhomogeneities are distant enough. Under this assumption, we derive an explicit formula for what we call "approximate" eigenelements of the limit far field operator F^0 (and thus of the limit time reversal operator T^0). Before stating this result, we first recall a classical result for oscillatory integrals that will be very useful for our analysis. This result, which can be found in [31, p. 348], is restated here in a slightly different form that is more convenient for our purposes.

Theorem 11. *Let S be a smooth hypersurface in $\mathbb{R}^N$ whose Gaussian curvature (i.e. the product of the principal curvatures) is nonzero everywhere and let $\psi \in \mathcal{C}_0^\infty(\mathbb{R}^N)$ such that Supp (ψ) intersects S in a compact subset of S. Then, as $|\boldsymbol{\xi}| \to +\infty$, we have*

$$\int_S \psi(\boldsymbol{\alpha})e^{i\boldsymbol{\alpha}\cdot\boldsymbol{\xi}}\,\mathrm{d}\boldsymbol{\alpha} = O(|\boldsymbol{\xi}|^{(1-N)/2}).$$

Theorem 12. *Let κ_p^ε and κ_p^μ be the contrasts defined by 4.3. For all $p = 1,\dots,M$ and all $\ell = 1,2,3$, we introduce the following functions of $L^2(S^2)$*

$$e_p(\boldsymbol{\alpha}) = e^{-ik\boldsymbol{\alpha}\cdot\boldsymbol{s}_p}, \qquad\qquad g_{p,\ell}(\boldsymbol{\alpha}) = h_{p,\ell}(\boldsymbol{\alpha})e_p(\boldsymbol{\alpha}),$$

where $h_{p,\ell} \in L^2(S^2)$ is an eigenfunction (with eigenvalue $\zeta_{p,\ell}$) of the compact self-adjoint integral operator $\mathcal{M}_p \in \mathcal{L}(L^2(S^2))$ (see statement (iv) in Lemma 10). We also set

$$\lambda_p^\varepsilon = -4\pi\kappa_p^\varepsilon|\mathcal{B}_p|, \qquad\qquad \lambda_{p,\ell}^\mu = \kappa_p^\mu\zeta_{p,\ell} \tag{4.9}$$

Then, we have the following two results.

(i) As $kd \to \infty$, the functions e_p satisfy

$$F^0 e_p = \lambda_p^\varepsilon e_p + O\left((kd)^{-1}\right). \tag{4.10}$$

(ii) As $kd \to \infty$, the functions $g_{p,\ell}$ satisfy

$$F^0 g_{p,\ell} = \lambda_{p,\ell}^\mu g_{p,\ell} + O\left((kd)^{-1}\right). \tag{4.11}$$

Proof. (i) We compute $F^0 e_p$ for a fixed $1 \le p \le M$. Thanks to 4.8, we have

$$(F^0 e_p)(\boldsymbol{\beta}) = \sum_{q=1}^{M} I_{pq}(\boldsymbol{\beta}) e_q(\boldsymbol{\beta})$$

in which $I_{pq}(\boldsymbol{\beta}) = \kappa_q^\mu \mathcal{M}_q(e_p\,\overline{e_q})(\boldsymbol{\beta}) - \kappa_q^\varepsilon |\mathcal{B}_q| (e_p, e_q)_{L^2(S^2)}$. According to 3.3, we note that for $q \neq p$, we have $(e_p, e_q)_{L^2(S^2)} = O\left((kd)^{-1}\right)$. On the other hand, Theorem 11 shows that for $q \neq p$, the integral $\mathcal{M}_q(e_p\,\overline{e_q})(\boldsymbol{\beta}) = \int_{S^2} (\boldsymbol{\beta} \cdot \mathbb{M}_q\, \boldsymbol{\alpha})\, e^{ik\boldsymbol{\alpha}\cdot(\boldsymbol{s}_q - \boldsymbol{s}_p)}\, \mathrm{d}\boldsymbol{\alpha}$ behaves like $O\left((kd)^{-1}\right)$. Consequently, for all $q \neq p$, we have $I_{pq}(\boldsymbol{\beta}) = O\left((kd)^{-1}\right)$ uniformly for all $\boldsymbol{\beta} \in S^2$. Concerning the diagonal term ($q = p$), we remark that for all $\boldsymbol{\beta} \in S^2$ ($\mathbb{1}$ is the constant function equal to 1)

$$\mathcal{M}_p(e_p\overline{e_p})(\boldsymbol{\beta}) = \mathcal{M}_p(\mathbb{1})(\boldsymbol{\beta}) = \int_{S^2} (\boldsymbol{\beta} \cdot \mathbb{M}_p\, \boldsymbol{\alpha})\, \mathrm{d}\boldsymbol{\alpha} = \boldsymbol{\beta} \cdot \mathbb{M}_p \int_{S^2} \boldsymbol{\alpha}\, \mathrm{d}\boldsymbol{\alpha} = 0. \tag{4.12}$$

Therefore, $I_{pp}(\boldsymbol{\beta}) = -4\pi\kappa_p^\varepsilon |\mathcal{B}_p| = \lambda_p^\varepsilon$ and hence $F^0 e_p = \lambda_p^\varepsilon e_p + O\left((kd)^{-1}\right)$, from which one easily gets 4.10.

(ii) Let $1 \le p \le M$ and $1 \le \ell \le 3$ be fixed. Using once again 4.8, we get that $(F^0 g_{p,\ell})(\boldsymbol{\beta}) = \sum_{q=1}^{M} I_{pq}(\boldsymbol{\beta}) e_q(\boldsymbol{\beta})$ where we have set now

$$I_{pq}(\boldsymbol{\beta}) = \kappa_q^\mu \mathcal{M}_q\left(h_{p,\ell}\, e_p\, \overline{e_q}\right)(\boldsymbol{\beta}) - \kappa_q^\varepsilon |\mathcal{B}_q| (h_{p,\ell} e_p, e_q)_{L^2(S^2)}.$$

For $q \neq p$ the two terms $(h_{p,\ell} e_p, e_q)_{L^2(S^2)}$ and $\mathcal{M}_q\left(h_{p,\ell} e_p\, \overline{e_q}\right)(\boldsymbol{\beta})$ are oscillatory integrals of the form given in Theorem 11. Therefore, $I_{pq}(\boldsymbol{\beta}) = O\left((kd)^{-1}\right)$ for $q \neq p$. On the other hand, for $q = p$, we see by Lemma 10, (iv), that

$$\begin{aligned} I_{pp}(\boldsymbol{\beta}) =& \kappa_p^\mu \mathcal{M}_p h_{p,\ell}(\boldsymbol{\beta}) - \kappa_p^\varepsilon |\mathcal{B}_p| (h_{p,\ell} e_p, e_p)_{L^2(S^2)} \\ =& \kappa_p^\mu \zeta_{p,\ell} h_{p,\ell}(\boldsymbol{\beta}) - \kappa_p^\varepsilon |\mathcal{B}_p| (h_{p,\ell}, \mathbb{1})_{L^2(S^2)}. \end{aligned}$$

By (4.12) we observe that $\mathbb{1}$ is in the null space of $\mathcal{M}_p$. Since $\mathcal{M}_p$ is self-adjoint, this yields $(h_{p,\ell}, \mathbb{1})_{L^2(S^2)} = \frac{1}{\zeta_{p,\ell}} (\mathcal{M}_p h_{p,\ell}, \mathbb{1})_{L^2(S^2)} = \frac{1}{\zeta_{p,\ell}} (h_{p,\ell}, \mathcal{M}_p \mathbb{1})_{L^2(S^2)} = 0$, and, thus, $I_{pp}(\boldsymbol{\beta}) = \kappa_p^\mu \zeta_{p,\ell} h_{p,\ell}(\boldsymbol{\beta})$ which concludes the proof. □

Remark 13. *We note that the approximate eigenfunctions of F^0 are the far fields corresponding to monopole or dipole sources located at the centers of the small inhomogeneities. More precisely, let $G(\boldsymbol{x}, \boldsymbol{y}) = \frac{e^{ik|\boldsymbol{x}-\boldsymbol{y}|}}{4\pi|\boldsymbol{x}-\boldsymbol{y}|}$ denote the outgoing Green's function of the Helmholtz operator in $\mathbb{R}^3$. Then, $e_p(\boldsymbol{\beta}) = e^{-ik\boldsymbol{\beta}\cdot\boldsymbol{s}_p}$ is nothing but the far field in the direction $\boldsymbol{\beta} \in S^2$ of the point source $G(\cdot, \boldsymbol{s}_p)$ located at $\boldsymbol{s}_p$. Similarly, the function $g_{p,\ell}(\boldsymbol{\beta}) = h_{p,\ell}(\boldsymbol{\beta})\, e_p(\boldsymbol{\beta}) = (\boldsymbol{\beta} \cdot V_{p,\ell})\, e^{-ik\boldsymbol{\beta}\cdot\boldsymbol{s}_p}$ represents the far field in the direction $\boldsymbol{\beta} \in S^2$ of the dipole source $\frac{1}{ik} \nabla G(\cdot, \boldsymbol{s}_p) \cdot V_{p,\ell}$ of direction $V_{p,\ell}$ located at $\boldsymbol{s}_p$.*

4.2 Justification of the DORT Method

We recall that the DORT method consists of the observation that eigenfunctions of the time-reversal operator possess selectively focusing properties. In the following section, we provide a precise signification of this property. We start with a straightforward consequence of Theorem 12 (see Remark 9), which provides the approximate eigenelements of the limit time reversal operator in the regime of uncoupled scatterers ($kd \to \infty$).

Corollary 14. *Under the notation of Theorem 12, we have the following estimates as* $kd \to \infty$

$$T^0 e_p = (\lambda_p^\varepsilon)^2 e_p + O\left((kd)^{-1}\right), \qquad T^0 g_{p,\ell} = (\lambda_{p,\ell}^\mu)^2 g_{p,\ell} + O\left((kd)^{-1}\right).$$

The next result shows that the above $4M$ approximate eigenfunctions e_p and $g_{p,\ell}$ for $p = 1, \dots, M$ and $\ell = 1, 2, 3$ span a subspace of dimension $4M$.

Proposition 15. *Under the notation of Theorem 12, the functions e_p and $g_{p,\ell}$ for $p = 1, \dots, M$ and $\ell = 1, 2, 3$ are linearly independent.*

Proof. Suppose that there exists complex coefficients $(a_p)_{p=1,\dots,M}$ and $(b_{p,\ell})_{p=1,\dots,M}^{j=1,2,3}$ such that

$$\sum_{p=1}^{M} a_p \, e_p(\boldsymbol{\beta}) + \sum_{p=1}^{M} \sum_{\ell=1}^{3} ik \, b_{p,\ell} \; g_{p,\ell}(\boldsymbol{\beta}) = 0, \qquad \forall \, \boldsymbol{\beta} \in S^2.$$

According to Remark 13, the above relation amounts to saying that the function $u(\boldsymbol{x}) := \sum_{p=1}^{M} a_p \, G(\boldsymbol{x}, \boldsymbol{s}_p) + \sum_{p=1}^{M} \sum_{\ell=1}^{3} b_{p,\ell} \nabla G(\boldsymbol{x}, \boldsymbol{s}_p) \cdot V_{p,\ell}$ has a vanishing far field. By Rellich's lemma, u must vanish everywhere, so that

$$\sum_{p=1}^{M} a_p \, G(\boldsymbol{x}, \boldsymbol{s}_p) + \sum_{p=1}^{M} \sum_{\ell=1}^{3} b_{p,\ell} \nabla G(\boldsymbol{x}, \boldsymbol{s}_p) \cdot V_{p,\ell} = 0, \qquad \forall \, \boldsymbol{x} \notin \{\boldsymbol{s}_1, \dots, \boldsymbol{s}_M\}. \tag{4.13}$$

Fix $q \in \{1, \dots, M\}$ and choose $\boldsymbol{x} = \boldsymbol{s}_q + \rho \widehat{\boldsymbol{x}}$, for $\widehat{\boldsymbol{x}} \in S^2$ and $0 \le \rho \le \rho^*$ small enough. Multiplying 4.13 by ρ^2 and taking the limit as $\rho \to 0$, we note that the only non vanishing contribution comes from the most singular term. More precisely, the dipole term corresponding to $p = q$ gives $\lim_{\rho \to 0} \rho^2 \nabla G(\boldsymbol{s}_q + \rho \widehat{\boldsymbol{x}}, \boldsymbol{s}_q) \cdot V_{q,\ell} = \dfrac{1}{4\pi} (\widehat{\boldsymbol{x}} \cdot V_{q,\ell})$. Therefore, $\widehat{\boldsymbol{x}} \cdot \left(\sum_{\ell=1}^{3} b_{q,\ell} V_{q,\ell} \right) = 0$. Since $\widehat{\boldsymbol{x}} \in S^2$ is arbitrary and since the vector columns $V_{q,1}, V_{q,2}$ and $V_{q,3}$ are linearly independent, the above relation yields $b_q^1 = b_q^2 = b_q^3 = 0$ for all $q \in \{1, \dots, M\}$. Finally, 4.13 reduces then to $\sum_{p=1}^{M} a_p G(\boldsymbol{x}, \boldsymbol{s}_p) = 0$ for all $\boldsymbol{x} \notin \{\boldsymbol{s}_1, \dots, \boldsymbol{s}_M\}$ from which one can easily get that $a_1 = \dots = a_M = 0$. □

Summing up, we have proved that in the regime of small and distant inhomogeneities ($\delta \ll \lambda_p \ll d$), the limit time reversal operator T^0 admits $4M$ eigenvalues : $(\lambda_p^\varepsilon)^2$, $(\lambda_{p,\ell}^\mu)^2$ for $p = 1, \dots, M$, $\ell = 1, 2, 3$. In order to complete our justification of the DORT method, we need to show that the corresponding (approximate) eigenfunctions e_p and $g_{p,\ell}$ generate incident waves focusing selectively on the inhomogeneities. Given p in $\{1, \dots, M\}$, let us first consider the incident Herglotz wave associated with a density e_p (TE eigenfunctions). Then, from (3.3), $u_{I,p}(\boldsymbol{x}) = O\left(|\boldsymbol{x} - \boldsymbol{s}_p|^{-1}\right)$. Regarding the TM eigenfunctions, the incident Herglotz wave associated with $g_{p,\ell} = h_{p,\ell} \, e_p$ is $u_{I,p,\ell}(\boldsymbol{x}) = \int_{S^2} e^{ik\boldsymbol{\alpha} \cdot (\boldsymbol{x} - \boldsymbol{s}_p)} h_{p,\ell}(\boldsymbol{\alpha}) \, \mathrm{d}\boldsymbol{\alpha}$, which behaves like $O\left((kd)^{-1}\right)$ from Theorem 11.

Remark 16. *Clearly, similar selective focusing results hold for the two dimensional problem. More precisely, by using once again Theorem 11 with $N = 2$, one can show that each inhomogeneity gives rise to 3 eigenvalues, one associated with the dielectric permittivity contrast and 2 with the magnetic permeability contrast. This is also confirmed by our numerical investigations, which are detailed in Section 6.*

Remark 17. *In the particular case of spherical inclusions, the polarization tensors become (see for example [3]) : $\mathbb{M}_p = 8\pi|\mathcal{B}_p|\frac{\mu_p}{\mu_p+\mu_0}\mathrm{I}$. One can then easily check that the TM eigenvalues $\lambda^{\mu}_{p,\ell}$ of the far field operator are given by relations 4.9, with $\zeta_{p,\ell} = 32\pi^2|\mathcal{B}_p|\,\frac{\mu_p}{\mu_p+\mu_0}$.*

5 Selective focusing for open time reversal mirrors

In this section, we investigate the case of an open TRM, *i.e.* the case where the TRM does not completely surround the inhomogeneities. For the sake of brevity, we will only stress the main differences with the case of a closed TRM. Let $\widehat{S} \subsetneq S^2$ denote the set of emission directions covered by the open TRM (and thus $-\widehat{S}$ represents the set of reception directions). We assume that the emission (resp. reception) directions of the open TRM are described by a smooth cutoff function $\chi_+ \in \mathcal{C}_0^\infty(S^2)$ (resp. $\chi_- \in \mathcal{C}_0^\infty(S^2)$) with $\operatorname{Supp}\chi_+ \subset \widehat{S}$ (resp. $\operatorname{Supp}\chi_- \subset -\widehat{S}$). The smoothness assumption on $\chi_\pm$ is purely technical and is used to derive more easily the asymptotic behavior of the oscillating integrals. However, our results still hold in the more realistic case where $\chi_\pm$ are characteristic functions of $\pm\widehat{S}$ (see Remark 23). Then, we define the far field operator corresponding to an open TRM by $\widehat{F} = P_- F P_+^* \in \mathcal{L}(L^2(\widehat{S}), L^2(-\widehat{S}))$, where $P_\pm : L^2(S^2) \to L^2(\pm\widehat{S})$ denote the restriction operators $P_\pm f = (\chi_\pm f)|_{\pm\widehat{S}}$ and $P_\pm^* : L^2(\pm\widehat{S}) \to L^2(S^2)$, whose adjoints are the extension operators by zero from $\pm\widehat{S}$ to S^2. Then, following the arguments detailed in [20, Sect. 5], one easily gets that for open TRM, the time reversal operator is once again of the form $\widehat{T} = \widehat{F}^*\widehat{F} \in \mathcal{L}(L^2(\widehat{S}))$, and is nothing but the integral operator with kernel $\widehat{t}(\boldsymbol{\alpha},\boldsymbol{\beta}) = \int_{-\widehat{S}} A(\boldsymbol{\alpha},\boldsymbol{\gamma})\,\overline{A(\boldsymbol{\beta},\boldsymbol{\gamma})}\,\mathrm{d}\boldsymbol{\gamma}$. Moreover, $\widehat{T}$ defines a compact positive and self-adjoint operator. Nevertheless, unlike the full far field operator F, the "finite aperture" far field operator $\widehat{F}$ is not anymore normal and the eigenfunctions of $\widehat{F}$ and $\widehat{T}$ are not necessary the same. Regarding the case of small inhomogeneities, the limit time reversal operator denoted $\widehat{T}^0 \in \mathcal{L}(L^2(\widehat{S}))$ is then the integral operator with kernel $\widehat{t}^{\,0}(\boldsymbol{\alpha},\boldsymbol{\beta}) = \int_{-\widehat{S}} A^0(\boldsymbol{\alpha},\boldsymbol{\gamma})\,\overline{A^0(\boldsymbol{\beta},\boldsymbol{\gamma})}\,\mathrm{d}\boldsymbol{\gamma}$ where A^0 is the limit scattering amplitude is given by 4.4. Then, given $\widehat{f} \in L^2(\widehat{S})$, the time reversal operator can be represented by

$$\begin{aligned}\widehat{T}^0\widehat{f}(\boldsymbol{\beta}) = \sum_{q=1}^{M}\Big\{\sum_{p=1}^{M}\int_{\widehat{S}}\Big(\int_{-\widehat{S}}&\Big[\kappa_p^\mu(\boldsymbol{\gamma}\cdot\mathbb{M}_p\boldsymbol{\alpha}) - \kappa_p^\varepsilon|\mathcal{B}_p|\Big] \\ &\Big[\kappa_q^\mu(\boldsymbol{\gamma}\cdot\mathbb{M}_q\boldsymbol{\beta}) - \kappa_q^\varepsilon|\mathcal{B}_q|\Big]\; e_p(\boldsymbol{\gamma})\,\overline{e_q(\boldsymbol{\gamma})}\,\mathrm{d}\boldsymbol{\gamma}\Big)\;\overline{e_p(\boldsymbol{\alpha})}\,\widehat{f}(\boldsymbol{\alpha})\,\mathrm{d}\boldsymbol{\alpha}\Big\}\,e_q(\boldsymbol{\beta}).\end{aligned} \tag{5.1}$$

Concerning the selective focusing properties, the main difference with the case of a closed TRM is that, unlike in 4.12, $\mathbb{1}$ is not anymore in the kernel of the integral operator $\mathcal{M}_p$ (or more exactly to its counterpart for finite aperture TRM). Indeed, the integral $\int_{\widehat{S}}(\boldsymbol{\beta}\cdot\mathbb{M}_p\,\boldsymbol{\alpha})\,\mathrm{d}\boldsymbol{\alpha}$ does not necessarily vanish for an arbitrary subset $\widehat{S} \subsetneq S^2$.

In the sequel, we consider successively the three cases : the purely TE case (i.e. $\kappa_p^\mu = 0$ for all $p = 1,\dots,M$), the purely TM case (i.e. $\kappa_p^\varepsilon = 0$ for all $p = 1,\dots,M$) and finally the mixed TE/TM case. For the latter case, we prove that the DORT method still works provided the TRM satisfies a symmetry condition (see 5.7).

We start with the case of vanishing magnetic contrast. One can prove the following result using the same arguments as those developed in [20, Sect. 5.2].

Theorem 18. *Let us assume that $\kappa_p^\mu = 0$ for all $p = 1, \dots, M$ (TE polarization). Then, as $kd \to \infty$, the functions $\widehat{e}_p(\boldsymbol{\alpha}) := (P_+ e_p)(\boldsymbol{\alpha}) = e^{-ik\boldsymbol{\alpha}\cdot\boldsymbol{s}_p}$, $\boldsymbol{\alpha} \in \widehat{S}$, are approximate eigenfunctions of $\widehat{T}^0$, in the sense that $\widehat{T}^0 \widehat{e}_p = (\widehat{\lambda}_p^\varepsilon)^2\, \widehat{e}_p + O\left((kd)^{-1}\right)$, with $\widehat{\lambda}_p^\varepsilon = \kappa_p^\varepsilon |\mathcal{B}_p|\, |\widehat{S}|$.*

Proof. In the case of vanishing contrast $\kappa_p^\mu = 0$ for all $p = 1, ..., M$, equation (5.1) reduces to

$$\widehat{T}^0 \widehat{f} = \sum_{p,q=1}^{M} \sum_{q=1}^{M} \kappa_p^\varepsilon \kappa_q^\varepsilon |\mathcal{B}_p||\mathcal{B}_q|\, (e_p, e_q)_{L^2(-\widehat{S})} (\widehat{f}, e_p)_{L^2(\widehat{S})} e_q.$$

Since χ_- is assumed to be a smooth function, we can still apply Theorem 11 and get that for $q \neq p$,

$$(e_p, e_q)_{L^2(-\widehat{S})} = O\left((kd)^{-1}\right), \tag{5.2}$$

which leads to $\widehat{T}^0 \widehat{e}_m = (\kappa_m^\varepsilon)^2 |\mathcal{B}_m|^2\, |\widehat{S}|^2\, \widehat{e}_m + O\left((kd)^{-1}\right)$. $\square$

In the case of purely TM polarization, i.e. when $\kappa_p^\varepsilon = 0$ for all of the inhomogeneities, we proceed similarly to the case of the closed time reversal mirror. That is, we shall see that the eigenfunctions of $\widehat{T}^0$ can be approximated using eigenfunctions of the integral operator $\widehat{\mathcal{M}}_p \in \mathcal{L}(L^2(\widehat{S}))$ with kernel

$$\widehat{m}_p(\boldsymbol{\alpha}, \boldsymbol{\beta}) := \int_{-\widehat{S}} (\boldsymbol{\gamma} \cdot \mathbb{M}_p \boldsymbol{\alpha})(\boldsymbol{\gamma} \cdot \mathbb{M}_p \boldsymbol{\beta})\, \mathrm{d}\boldsymbol{\gamma}. \tag{5.3}$$

The next Lemma, given without proof, summarizes some simple properties of the integral operator $\widehat{\mathcal{M}}_p$.

Lemma 19. *The following assertions hold true.*

(i) $\widehat{\mathcal{M}}_p \in \mathcal{L}(L^2(S^2))$ is a positive self-adjoint compact operator and hence it is diagonalizable.

(ii) $\widehat{\mathcal{M}}_p$ is a finite rank operator : $\operatorname{Rank} \mathcal{M}_p \leq 3$. *In particular, $\widehat{\mathcal{M}}_p$ admits at most 3 non zero eigenvalues $\widehat{\zeta}_{p,\ell}$, $\ell = 1, 2, 3$.*

Theorem 20. *Let $\kappa_p^\varepsilon = 0$ for all $p = 1, ..., M$ and let $\widehat{h}_{p,\ell} \in L^2(\widehat{S})$ be an eigenfunction of the compact self-adjoint integral operator $\widehat{\mathcal{M}}_p$ with kernel (5.3), associated with an eigenvalue $\widehat{\zeta}_{p,\ell} \neq 0$ for $\ell = 1, 2, 3$. Then, as $kd \to \infty$, the function*

$$\widehat{g}_{p,\ell}(\boldsymbol{\alpha}) = \widehat{h}_{p,\ell}(\boldsymbol{\alpha}) \widehat{e}_p(\boldsymbol{\alpha}), \qquad \forall\, \boldsymbol{\alpha} \in \widehat{S} \tag{5.4}$$

is an approximate eigenfunction of $\widehat{T}^0$, in the sense that

$$\widehat{T}^0 \widehat{g}_{p,\ell} = (\widehat{\lambda}_{p,\ell}^\mu)^2\, \widehat{g}_{p,\ell} + O\left((kd)^{-1}\right),$$

with $\widehat{\lambda}_{p,\ell}^\mu = \kappa_p^\mu \widehat{\zeta}_{p,\ell}$.

Proof. From (5.1) and for $\kappa_p^\varepsilon = 0$ for all $p = 1, \dots, M$, we have

$$\widehat{T}^0 \widehat{f}(\boldsymbol{\beta}) = \sum_{p,q=1}^{M} \kappa_q^\mu \kappa_p^\mu \int_{\widehat{S}} \boldsymbol{\alpha} \cdot \left[\int_{-\widehat{S}} \mathbb{M}_p \boldsymbol{\gamma} \, (\boldsymbol{\gamma} \cdot \mathbb{M}_q \boldsymbol{\beta}) \, e_p(\boldsymbol{\gamma}) \, \overline{e_q(\boldsymbol{\gamma})} \, \mathrm{d}\boldsymbol{\gamma} \right] \overline{e_p(\boldsymbol{\alpha})} \widehat{f}(\boldsymbol{\alpha}) \, \mathrm{d}\boldsymbol{\alpha} \, e_q(\boldsymbol{\beta}).$$

For $q \neq p$ the inner integral behaves like $O\left((kd)^{-1}\right)$ by Theorem 11. Thus, the time reversal operator can be represented by

$$\widehat{T}^0 \widehat{f} = \sum_{p=1}^{M} (\kappa_p^\mu)^2 \widehat{\mathcal{M}}_p \left(\widehat{f} \; \overline{\widehat{e}_p} \right) \widehat{e}_p + O\left((kd)^{-1} \right), \tag{5.5}$$

Noting that, for $m \neq p$,

$$\widehat{\mathcal{M}}_p \left(\widehat{h}_{m,\ell} \widehat{e}_m \; \overline{\widehat{e}_p} \right)(\boldsymbol{\beta}) = O\left((kd)^{-1} \right), \tag{5.6}$$

the statement follows immediately from the representation (5.5) of $\widehat{T}^0$ and the circumstance that $\widehat{h}_p$ is an eigenfunction of the integral operator $\widehat{\mathcal{M}}_p$. $\square$

In the case of mixed TE/TM polarization (*i.e.* when both contrasts are present), the following statement shows that for particular shapes of $\widehat{S}$, we can still obtain expressions of approximate eigenfunctions of the limit time reversal operator.

Theorem 21. *Let $\widehat{S}$ be chosen such that*

$$\int_{\widehat{S}} \boldsymbol{\alpha} \, \mathrm{d}\boldsymbol{\alpha} = 0. \tag{5.7}$$

Then, as $kd \to \infty$, the functions $\widehat{e}_p$ and $\widehat{g}_{p,\ell}$, $p = 1, ..., M$, respectively defined in Theorem 18 and Theorem 20, constitute approximate eigenfunctions of $\widehat{T}^0$ with an error bound of size $O\left((kd)^{-1}\right)$.

Proof. For the functions $\widehat{e}_\ell$, $\ell = 1, ..., M$, the statement is a result of the representation (5.1), the assumption that the integral $\int_{\widehat{S}} \boldsymbol{\alpha} \, \mathrm{d}\boldsymbol{\alpha}$ vanishes and Theorem 11. In particular, we have

$$\begin{aligned}
\widehat{T}^0 \widehat{e}_\ell(\boldsymbol{\beta}) =& (\kappa_\ell^\varepsilon)^2 |\mathcal{B}_\ell|^2 \, |\widehat{S}| \, \widehat{e}_\ell(\boldsymbol{\beta}) + \sum_{p=1}^{M} (\kappa_p^\mu)^2 \widehat{\mathcal{M}}_p \Big(\widehat{e}_\ell \, \overline{\widehat{e}_p} \Big)(\boldsymbol{\beta}) \, e_p(\boldsymbol{\beta}) + O\left((kd)^{-1} \right) \\
&- \sum_{p,q=1}^{M} \kappa_p^\mu \kappa_q^\varepsilon |\mathcal{B}_q| \int_{\widehat{S}} \left(\int_{-\widehat{S}} (\boldsymbol{\gamma} \cdot \mathbb{M}_p \boldsymbol{\alpha}) \, e_p(\boldsymbol{\gamma}) \, \overline{e_q(\boldsymbol{\gamma})} \, \mathrm{d}\boldsymbol{\gamma} \right) \overline{e_p(\boldsymbol{\alpha})} \, \widehat{e}_\ell(\boldsymbol{\alpha}) \, \mathrm{d}\boldsymbol{\alpha} \, e_q(\boldsymbol{\beta}) \\
&- \sum_{p,q=1}^{M} \kappa_q^\mu \kappa_p^\varepsilon |\mathcal{B}_p| \int_{\widehat{S}} \left(\int_{-\widehat{S}} (\boldsymbol{\gamma} \cdot \mathbb{M}_q \boldsymbol{\beta}) \, e_p(\boldsymbol{\gamma}) \, \overline{e_q(\boldsymbol{\gamma})} \, \mathrm{d}\boldsymbol{\gamma} \right) \overline{e_p(\boldsymbol{\alpha})} \, \widehat{e}_\ell(\boldsymbol{\alpha}) \, \mathrm{d}\boldsymbol{\alpha} \, e_q(\boldsymbol{\beta}).
\end{aligned}$$

Using for $p \neq q$ Theorem 11, we find that

$$\int_{-\widehat{S}} \boldsymbol{\gamma} \, e_p(\boldsymbol{\gamma}) \, \overline{e_q(\boldsymbol{\gamma})} \, \mathrm{d}\boldsymbol{\gamma} = O\left((kd)^{-1} \right), \tag{5.8}$$

Hence, for $kd \to \infty$, the two double sums simplify respectively into

$$-\sum_{p=1}^{M} \kappa_p^\mu \kappa_p^\varepsilon |\mathcal{B}_p| \int_{\widehat{S}} \boldsymbol{\alpha} \cdot \mathbb{M}_p \left(\int_{-\widehat{S}} \boldsymbol{\gamma} \, \mathrm{d}\boldsymbol{\gamma} \right) \overline{\widehat{e}_p(\boldsymbol{\alpha})} \; \widehat{e}_\ell(\boldsymbol{\alpha}) \, \mathrm{d}\boldsymbol{\alpha} \; e_p(\boldsymbol{\beta}) + O\left((kd)^{-1} \right),$$

and

$$-\sum_{p=1}^{M}\kappa_p^{\mu}\kappa_p^{\varepsilon}|\mathcal{B}_p|\int_{\widehat{S}}\boldsymbol{\beta}\cdot\mathbb{M}_p\left(\int_{-\widehat{S}}\boldsymbol{\gamma}\,\mathrm{d}\boldsymbol{\gamma}\right)\overline{\widehat{e_p}(\boldsymbol{\alpha})}\widehat{e}_\ell(\boldsymbol{\alpha})\,\mathrm{d}\boldsymbol{\alpha}\;e_p(\boldsymbol{\beta})+O\left((kd)^{-1}\right).$$

Thus, we have

$$\begin{aligned}\widehat{T}^0\widehat{e}_\ell(\boldsymbol{\beta})=&(\kappa_\ell^{\varepsilon})^2|\mathcal{B}_\ell|^2\,|\widehat{S}|\,\widehat{e}_\ell(\boldsymbol{\beta})+\sum_{p=1}^{M}(\kappa_p^{\mu})^2\widehat{\mathcal{M}}_p\left(\widehat{e}_\ell\,\overline{\widehat{e}_p}\right)(\boldsymbol{\beta})\,e_p(\boldsymbol{\beta})\\&-\sum_{p=1}^{M}\kappa_p^{\mu}\kappa_p^{\varepsilon}|\mathcal{B}_p|\int_{\widehat{S}}(\boldsymbol{\alpha}+\boldsymbol{\beta})\cdot\mathbb{M}_p\left(\int_{-\widehat{S}}\boldsymbol{\gamma}\,\mathrm{d}\boldsymbol{\gamma}\right)\overline{e_p(\boldsymbol{\alpha})}\,\widehat{e}_\ell(\boldsymbol{\alpha})\,\mathrm{d}\boldsymbol{\alpha}\;e_p(\boldsymbol{\beta})\\&+O\left((kd)^{-1}\right)\end{aligned}$$

By 5.7, we obtain

$$\widehat{T}^0\widehat{e}_\ell(\boldsymbol{\beta})=(\kappa_\ell^{\varepsilon})^2|\mathcal{B}_\ell|^2\,|\widehat{S}|\,\widehat{e}_\ell(\boldsymbol{\beta})+\sum_{p=1}^{M}(\kappa_p^{\mu})^2\widehat{\mathcal{M}}_p\left(\widehat{e}_\ell\,\overline{\widehat{e}_p}\right)(\boldsymbol{\beta})\,e_p(\boldsymbol{\beta})+O\left((kd)^{-1}\right).$$

But from Theorem 11

$$\widehat{\mathcal{M}}_p\left(\widehat{e}_\ell\,\overline{\widehat{e}_p}\right)(\boldsymbol{\beta})=\begin{cases}O\left((kd)^{-1}\right), & p\neq\ell,\\ \widehat{\mathcal{M}}_p\left(P_+\mathbb{1}\right)(\boldsymbol{\beta}), & p=\ell,\end{cases}$$

Moreover, from assumption 5.7, $P_+\mathbb{1}$ is in the null space of the integral operator $\widehat{\mathcal{M}}_p$. Hence, $\widehat{T}^0\widehat{e}_\ell(\boldsymbol{\beta})=(\kappa_\ell^{\varepsilon})^2|\mathcal{B}_\ell|^2\,|\widehat{S}|\,\widehat{e}_\ell(\boldsymbol{\beta})+O\left((kd)^{-1}\right)$.

Let $m\in 1,...,M$ be fixed. For the functions $\widehat{g}_{m,\ell}$ defined in (5.4), according to the representation (5.1) we obtain

$$\begin{aligned}&\widehat{T}^0\widehat{g}_{m,\ell}(\boldsymbol{\beta})\\=&\sum_{p=1}^{M}(\kappa_p^{\mu})^2\widehat{\mathcal{M}}_p\left(\widehat{g}_{m,\ell}\,\overline{\widehat{e}_p}\right)(\boldsymbol{\beta})\,e_p(\boldsymbol{\beta})+(\kappa_p^{\varepsilon})^2|\mathcal{B}_p|^2\,|\widehat{S}|\,\left(\widehat{g}_{m,\ell},e_p\right)_{L^2(\widehat{S})}e_p(\boldsymbol{\beta})\\&-\sum_{p=1}^{M}\sum_{q=1}^{M}\kappa_p^{\mu}\kappa_q^{\varepsilon}|\mathcal{B}_q|\int_{\widehat{S}}\left(\int_{-\widehat{S}}(\boldsymbol{\gamma}\cdot\mathbb{M}_p\boldsymbol{\alpha})e_p(\boldsymbol{\gamma})\,\overline{e_q(\boldsymbol{\gamma})}\,\mathrm{d}\boldsymbol{\gamma}\right)\overline{e_p(\boldsymbol{\alpha})}\;\widehat{g}_{m,\ell}(\boldsymbol{\alpha})\,\mathrm{d}\boldsymbol{\alpha}\,e_q(\boldsymbol{\beta})\\&-\sum_{p=1}^{M}\sum_{q=1}^{M}\kappa_q^{\mu}\kappa_p^{\varepsilon}|\mathcal{B}_p|\int_{\widehat{S}}\left(\int_{-\widehat{S}}(\boldsymbol{\gamma}\cdot\mathbb{M}_q\boldsymbol{\beta})\,e_p(\boldsymbol{\gamma})\,\overline{e_q(\boldsymbol{\gamma})}\,\mathrm{d}\boldsymbol{\gamma}\right)\overline{e_p(\boldsymbol{\alpha})}\,\widehat{g}_{m,\ell}(\boldsymbol{\alpha})\,\mathrm{d}\boldsymbol{\alpha}\,e_q(\boldsymbol{\beta})\\&+O\Big((kd)^{-1}\Big)\end{aligned}$$

Since $P_+\mathbb{1}\in\operatorname{Ker}\widehat{\mathcal{M}}_p$, $\left(\widehat{h}_{m,\ell},P_+\mathbb{1}\right)_{L^2(\widehat{S})}=\frac{1}{\zeta_{m,\ell}}\left(\widehat{h}_{m,\ell},\widehat{\mathcal{M}}_mP_+\mathbb{1}\right)_{L^2(\widehat{S})}=0$, we get like above that

$$\left(\widehat{g}_{m,\ell},e_p\right)_{L^2(\widehat{S})}=\left(\widehat{h}_{m,\ell}e_m,e_p\right)_{L^2(\widehat{S})}=\begin{cases}O\left((kd)^{-1}\right), & m\neq p,\\ 0, & m=p,\end{cases}$$

and hence $\widehat{T}^0\widehat{g}_{m,\ell}=(\kappa_m^{\mu})^2\zeta_{m,\ell}\widehat{g}_{m,\ell}+O\left((kd)^{-1}\right)$. □

In order to justify the DORT method for the case of open and symmetric mirrors, it remains to show that the functions $\widehat{e}_p$ and $\widehat{g}_{p,\ell}$ generate incident waves focusing selectively on the inhomogeneities. Given a fixed p in $\{1, \ldots, M\}$, let us first consider the incident Herglotz wave associated with a density $\widehat{e}_p$ (TE eigenfunctions). From (5.2) we immediately see that $u_{I,p}$ decreases like $|\boldsymbol{x} - \boldsymbol{s}_p|^{-1}$. Regarding the TM eigenfunctions, the incident Herglotz wave associated with $\widehat{g}_{p,\ell} = \widehat{h}_{p,\ell}\, \widehat{e}_p$ is an oscillatory integral given by $u_{I,p,\ell}(\boldsymbol{x}) = \int_{\widehat{S}} \widehat{h}_{p,\ell}(\boldsymbol{\alpha}) e^{ik\boldsymbol{\alpha}\cdot(\boldsymbol{x}-\boldsymbol{s}_p)}\, \mathrm{d}\boldsymbol{\alpha} = O\left((k|\boldsymbol{x} - \boldsymbol{s}_p|)^{-1}\right)$.

Remark 22. *Condition (5.7) is satisfied whenever $\widehat{S}$ is symmetric i.e. $\widehat{S} = -\widehat{S}$. Its main advantage lies in the fact that it allows us to decouple between the TE and TM approximate eigenfunctions $\widehat{e}_p$ and $\widehat{g}_{p,\ell}$. Nevertheless, numerical experiments indicate that selective focusing still holds for open TRM even when 5.7 is not satisfied (see Section 6). Unfortunately, we have not been able to prove this result.*

Remark 23. *We have assumed the open TRM to be described by a smooth cutoff function, so that we can apply directly Theorem 11. Of course, it would be more relevant for practical applications to assume the TRM to be defined via the characteristic function $\mathbb{1}|_{\pm\widehat{S}}$. In this case, one has to derive high frequency asymptotics (i.e. for $k \to +\infty$) of integrals of the form $\int_{\widehat{S}} \widehat{\psi}(\boldsymbol{\alpha}) e^{ik\boldsymbol{\alpha}\cdot\boldsymbol{s}}\, \mathrm{d}\boldsymbol{\alpha}$. Describing the TRM by spherical coordinates $\widehat{S} = \{\boldsymbol{\alpha} = (\theta, \varphi) \in J_\theta \times J_\varphi\}$, the above integral reduces to two dimensional oscillatory integrals of the form $\int_{J_\theta} \int_{J_\varphi} \Psi(\theta, \varphi) e^{ik\Phi_{\boldsymbol{s}}(\theta,\varphi)}\, \mathrm{d}\theta \mathrm{d}\varphi$. Using a two dimensional version of the stationary phase theorem [34, Chap. VIII], one can show that the above integrals decay as $k \to \infty$, with a rate of decay of $1/k$ (as in the case of a smooth TRM). This is due to the fact that the possible (interior) critical points of $\Phi_{\boldsymbol{s}}$ are non degenerate as it can be checked from lengthy but not difficult calculations.*

6 Numerical tests

We consider the case of spherical two-dimensional inclusions, i.e. $\partial\mathcal{B}_p = \boldsymbol{s}_p + a_p S^2, \quad p = 1, ..., M$, where a_p denotes the radius of the disk $\mathcal{B}_p$. We use an integral equation approach to solve the scattering problem (4.2). Taking advantage of the particular form of the inhomogeneities, we use a spectral approach (also known as multipole expansion or Mie series method) to solve the system of integral equations (instead of a using a boundary element method). Each boundary unknown density is then decomposed on the local Fourier basis associated to each inhomogeneity. Using the projection of the integral operators in these Fourier basis, it is possible to obtain an explicit expression for the integral kernels, for more details see for instance [27, 32]. This leads to solving a linear system whose diagonal blocks represent single scattering, while the off-diagonal blocks take into account multiple scattering phenomena. The above method can be adapted to tackle the three-dimensional case, the unknown density being then approximated via an infinite sum of spherical harmonics. Of course, this leads to much larger systems to solve (more details on the case of non penetrable scatterers can be found for instance in [19]).

We illustrate the DORT method for several different setups. The implementation was realized under MATLAB. Throughout this section we assume that $\mu_0 = \varepsilon_0 = 1$ (which is equivalent to considering ε and μ as being not the absolute but the relative permittivity and permeability) and $\omega = 2\pi$, leading to a wavelength $\lambda = 1$. The radius of the spheres is given by $a_p = 0.002$ for all $p = 1, ..., M$. The emission and reception directions are obtained by discretizing uniformly the unit circle $(0, 2\pi)$ using 200 points. These directions will be fixed and in the case of an open TRM, we will restrict ourselves to those emission and reception directions which are in the interior of the given set $\widehat{S}$ resp. $-\widehat{S}$. We begin with an example of one single inclusion. Then, we proceed by an example with two inclusions, by considering successively a symmetric and a non symmetric configuration (i.e. two inclusions different magnetic and dielectric contrast). More realistic setups (with an open TRM and noise) are presented in Examples 3a and 3b.

Example 1. One inclusion. We first consider the case of one single inclusion, and we show in Table 1 the four largest eigenvalues of the time-reversal operator for different values of the dielectric and magnetic contrasts. In particular, we observe that for each setup, there are three significant eigenvalues, two of them being equal. These eigenvalues correspond to the TM polarization (magnetic contrast) while the third one is related to the TE polarization (dielectric contrast). This fact is in agreement with the DORT method in dimension two (see Remark 16).

μ_1	ε_1	λ_1	λ_2	λ_3	λ_4
4	2	0.0049019	0.0017636	0.0017636	6.8683e-13
5	1.5	0.0021772	0.0021772	0.0012253	8.4791e-13

Table 1: Single inclusion at position $s_1 = (0, 5)$. We present the different eigenvalues of the time-reversal operator (rescaled by a factor $1/|\mathcal{B}_1| = 1/(\pi a_1^2)$).

Figure 1 shows the absolute values of the DORT Herglotz waves for the case $\mu_1 = 4$ and $\varepsilon_1 = 2$. We see that the Herglotz wave function associated to these eigenvalues represents a dipole situated at the (unknown) location of the inclusion. Also, the first Herglotz wave associated to the largest eigenvalue is a monopole, which confirms our theoretical results. In Figure 2 we present similar results for the case $\mu_1 = 5$ and $\varepsilon_1 = 1.5$. Here, the first two eigenvalues are equal, see Table 1, and hence, they are most likely associated to the magnetic contrast. Indeed, as we can see in Figure 2, the first two Herglotz waves are dipoles whereas the third is a monopole situated at the unknown location of the inclusion.

Example 2a. Two non symmetric inclusions. We consider a second inclusion at position $(10, 22)$ with the same size as inclusion $\mathcal{B}_1$ and with $\varepsilon_2 = 3$ and $\mu_2 = 15$. In Figure 3 one can see that the first six eigenvalues (ordered by their magnitude) of the time-reversal mirror are significantly larger than the subsequent eigenvalues. Moreover, the second and third as well as the fourth and fifth eigenvalues are equal. This indicates that the Herglotz waves associated to the 2nd and third eigenvalue are dipoles focusing on one inclusion and that the Herglotz waves generated from the 4th and 5th eigenfunctions should focus on the other inclusion. Indeed, as can be seen in Figure 4, this is the case. Also, the first and six Herglotz waves are monopoles each focusing on one of the two inclusions which is what one expects from the theoretical results.

Example 2b. Two symmetric inclusions. Let us again consider the two inclusions $\mathcal{B}_1$ and $\mathcal{B}_2$ at $(0, 5)$ and $(10, 22)$ but with the same magnetic and dielectric contrast given by $\varepsilon_1 = \varepsilon_2 = 3$ and $\mu_1 = \mu_2 = 5$. In Figure 5 the obtained eigenvalues are shown.

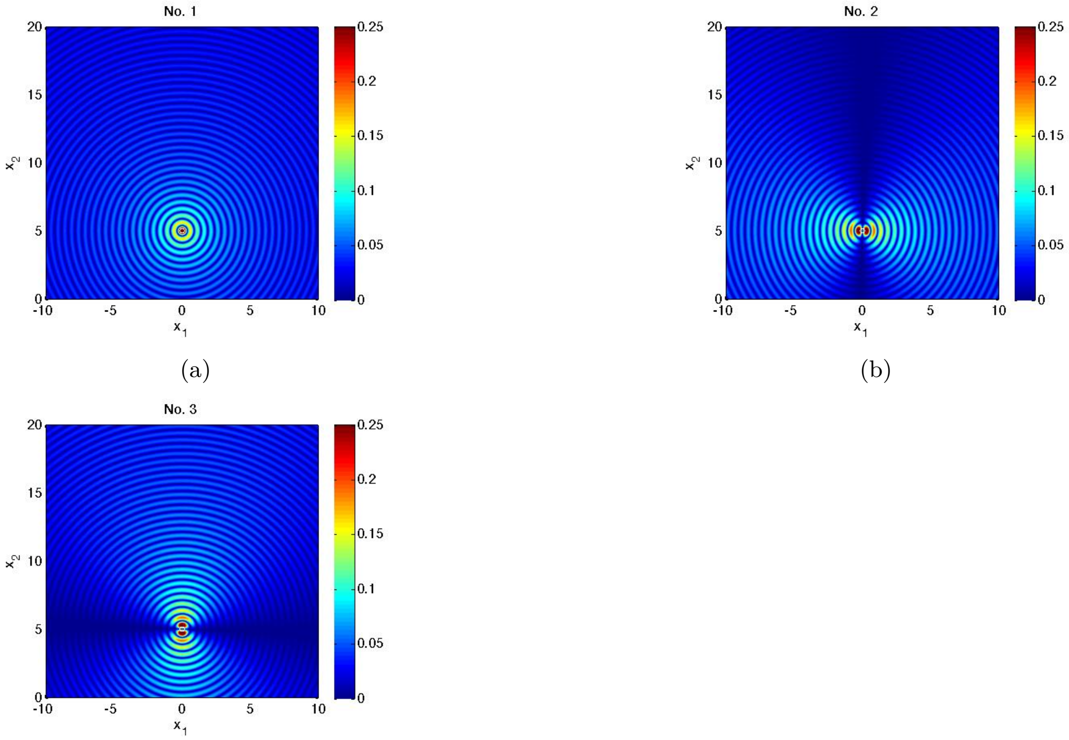

(a) (b) (c)

Figure 1: Herglotz waves (in modulus) generated by the eigenfunctions of the time reversal operator for parameters $\mu_1 = 4$ and $\varepsilon_1 = 2$. (a) uses the eigenfunction of the first eigenvalue, (b) of the second and (c) of the third eigenvalue.

The absolute values of the associated Herglotz waves is presented in Figures 6(a)–(f). Noting that the eigenvalues associated to $\mathcal{B}_1$ equal those associated to $\mathcal{B}_2$, there are two of the first six (associated to the first six largest eigenvalues) eigenelements of T^0 which are in span$\{e_1, e_2\}$, further two are in span$\{g_{1,\ell},\ \ell = 1, 2\}$, and the remaining two are in span$\{g_{2,\ell},\ \ell = 1, 2\}$. In particular, this explains the observation that the Herglotz waves do not selectively focus on one but on both of the inclusions. Nevertheless, selective focusing can be recovered by using a linear combination of the Herglotz waves using Figure 6, as proposed in Prada *et al.* [30]. For example, in Figure 7(a), we present the absolute value of the first Herglotz function plus i-times the second Herglotz wave function. In Figure 7(b), we plot i-times the third Herglotz waves minus the sixth Herglotz wave focuses on $\mathcal{B}_1$.

Example 3a. Two non symmetric inclusions with an open symmetric TRM. In this example we use the same setup as in Example 2a, but with an open and symmetric TRM given by

$$\widehat{S}_{sym} = \{\boldsymbol{\alpha} \in S^2 : \boldsymbol{\alpha} = (\cos\phi, \sin\phi),\ \phi \in [\pi/5, 4\pi/5] \cap \pi + [\pi/5, 4\pi/5]\}. \tag{6.1}$$

Furthermore, we consider the more realistic setup of working with noisy data. In Figure 8 we present the eigenvalues obtained from using the open symmetric TRM (6.1) for different levels of noise. Whereas the first six eigenvalues do not seem to depend on the amount

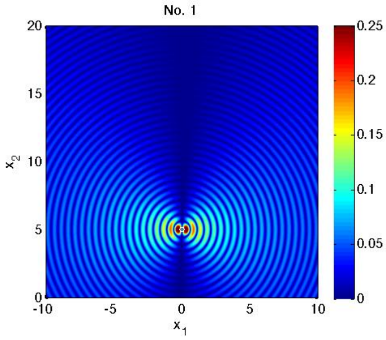

(a)

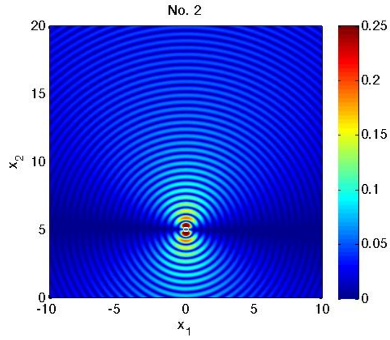

(b)

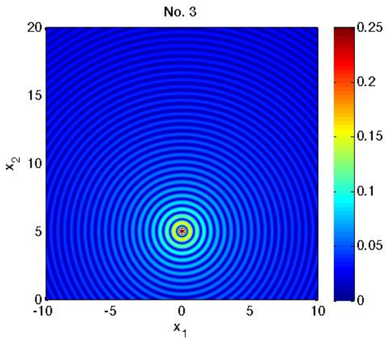

(c)

Figure 2: Same as Figure 1, but with a strong magnetic contrast.

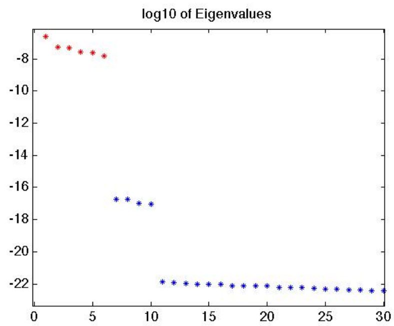

Figure 3: Eigenvalues of the time-reversal operator obtained for the setup of Example 2a.

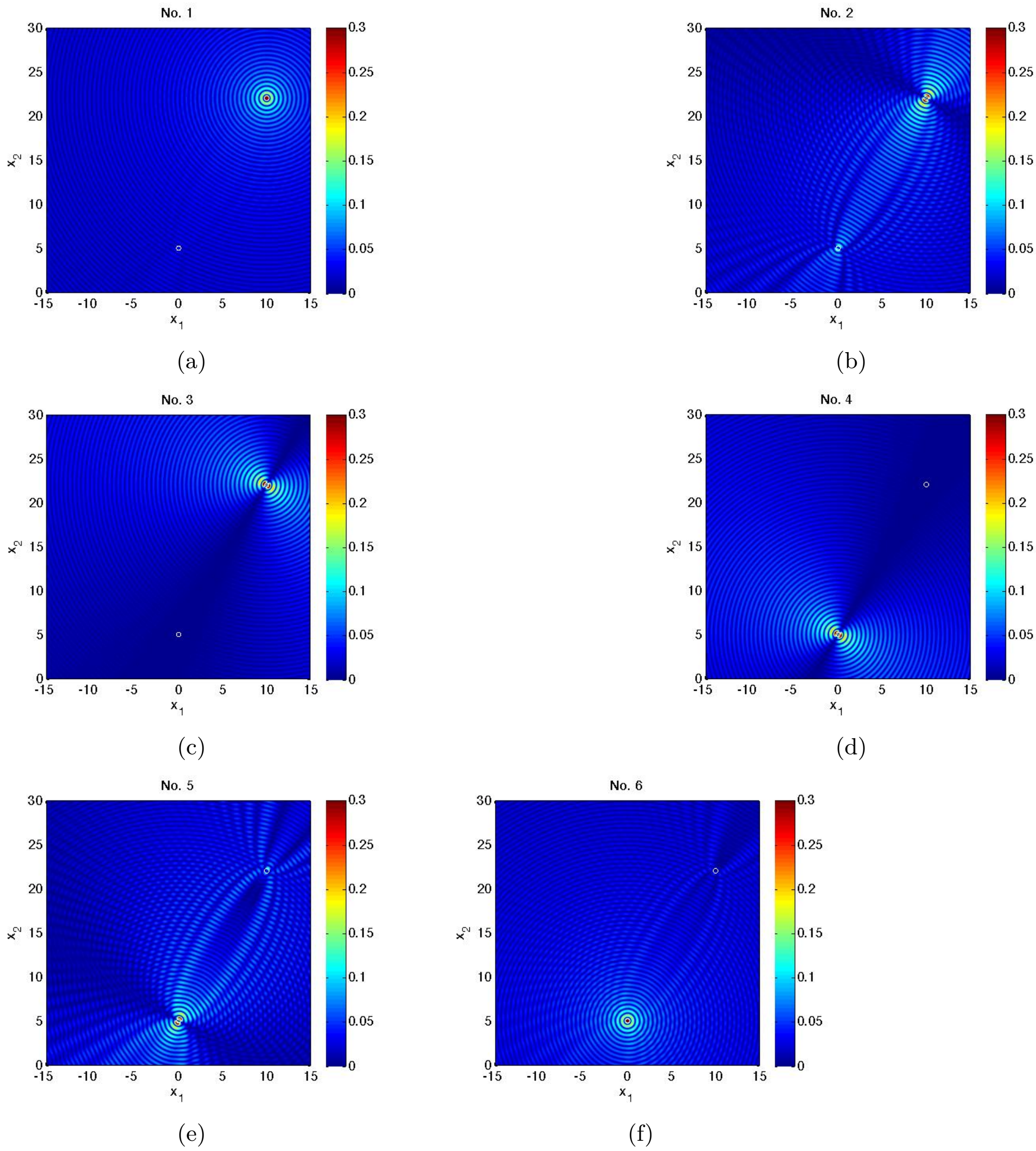

Figure 4: Two inclusions with different magnetic and dielectric contrast (Example 2a).

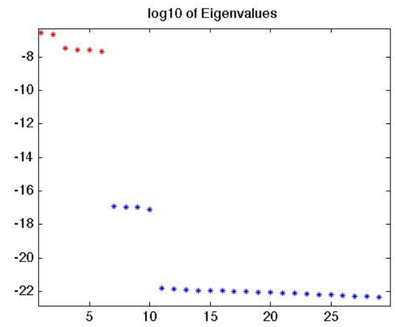

Figure 5: Eigenvalues of the time-reversal operator obtained for the setup of Example 2b.

of noise, the subsequent eigenvalues are significantly larger when working with noise. In Figure 9 the absolute values of the associated Herglotz waves are shown for a noise of 8%. Although the first six eigenvalues are not anymore significant larger than the subsequent eigenvalues, the associated Herglotz waves still focus selectively. This is even true in the case of 20% of noise, compare Figure 10.

Example 3b. Two non symmetric inclusions with an open and non symmetric TRM. In this last example we study the case of a non symmetric open TRM given by

$$\widehat{S}_{non-sym} = \{\boldsymbol{\alpha} \in S^2 : \boldsymbol{\alpha} = (\cos\phi, \sin\phi),\ \phi \in [\pi/5, 4\pi/5]\}. \tag{6.2}$$

We recall that the open but non symmetric TRM did not allow a direct decoupling of the TE- and TM-eigenfunctions, see Remark 22. Nevertheless, it is straightforard to see that all eigenfunctions are linear combinations of monopoles and dipoles with centres $\boldsymbol{s}_p$, $p = 1, ..., M$ up to an error of order $O((kd)^{-1})$. In this numerical example, we use the same setup as in Example 2a (i.e. the same position, size and contrasts of the inclusions). Our numerical experiment indicates that the DORT method still works. We present the eigenvalues in Figure 11 without and with noise. Using noisy data (8% noise added to the far field data) we obtain the Herglotz waves presented in Figure 12, which do still selectively focus on the inclusions.

7 Conclusion

In this work, we presented a rigorous mathematical justification of the DORT method in the context of penetrable small inhomogeneities. The mathematical model used to achieve this analysis is a far field model for time reversal in the frequency domain. The main result states that each scatterer gives rise to $N + 1$ significant eigenvalues (N being the dimension), provided the scatterers are small and distant enough. This result was proved for closed mirrors, but also for symmetric finite aperture mirrors. In the two-dimensional case, the theoretical results were further confirmed by numerical simulations. The case of non symmetric open mirrors requires further analysis and it not addressed in this paper.

Acknowledgments

The authors want to thank Bertrand Thierry for his contribution to the MATLAB code realizing the DORT method for penetrable spheres. They also thank Marc Bonnet (POems group, CNRS/Inria/Ensta) for his careful reading of this work and for pointing out to us a little sign mistake in the far field asymptotics. Support for this work was provided by the FRAE (`http://www.fnrae.org/`), research project IPPON.

References

[1] M. Abramowitz and I. A. Stegun, *Handbook of mathematical functions with formulas, graphs, and mathematical tables*, vol. 55 of National Bureau of Standards Applied Mathematics Series, U.S. Government Printing Office, Washington, D.C., 1964.

[2] H. Ammari, E. Iakovleva, D. Lesselier, and G. Perrusson, *Music-type electromagnetic imaging of a collection of small three-dimensional inclusions*, SIAM J. Sci. Comput., 29 (2007), pp. 674–709 (electronic).

[3] H. Ammari, E. Iakovleva, and S. Moskow, *Recovery of small inhomogeneities from the scattering amplitude at a fixed frequency*, SIAM J. Math. Anal., 34 (2003), pp. 882–900.

[4] X. Antoine, B. Pinçon, K. Ramdani, and B. Thierry, *Far field modeling of electromagnetic time reversal and application to selective focusing on small scatterers*, SIAM J. Appl. Math., 69 (2008), pp. 830–844.

[5] T. Arens, A. Lechleiter, and D. R. Luke, *Music for extended scatterers as an instance of the factorization method*, SIAM J. Appl. Math., 70 (2009), pp. 1283–1304.

[6] C. Ben Amar, N. Gmati, C. Hazard, and K. Ramdani, *Numerical simulation of acoustic time reversal mirrors*, SIAM J. Appl. Math., 67 (2007), pp. 777–791.

[7] L. Borcea, G. Papanicolaou, and F. G. Vasquez, *Edge illumination and imaging of extended reflectors*, SIAM J. Imaging Sciences, 1 (2008), pp. 75–114.

[8] D. H. Chambers and J. G. Berryman, *Target characterization using decomposition of the time-reversal operator: electromagnetic scattering from small ellipsoids*, Inverse Problems, 22 (2006), pp. 2145–2163.

[9] Q. Chen, H. Haddar, A. Lechleiter, and P. Monk, *A sampling method for inverse scattering in the time domain*, Inverse Problems, 26 (2010), p. 085001.

[10] M. Cheney, *The linear sampling method and the MUSIC algorithm*, Inverse Problems, 17 (2001), pp. 591–595.

[11] D. Colton, H. Haddar, and M. Piana, *The linear sampling method in inverse electromagnetic scattering theory*, Inverse Problems, 19 (2003), pp. S105–S137.

[12] D. Colton and A. Kirsch, *A simple method for solving inverse scattering problems in the resonance region*, Inverse Problems, 12 (1996), pp. 383–393.

[13] D. Colton and R. Kress, *Inverse acoustic and electromagnetic scattering theory*, vol. 93 of Applied Mathematical Sciences, Springer-Verlag, Berlin, second ed., 1998.

[14] A. Devaney, E. Marengo, and F. Gruber, *Time-reversal-based imaging and inverse scattering of multiply scattering point targets*, J. Acoust. Soc. Amer., 118 (2005), pp. 3129–3138.

[15] A. Fannjiang, *On time reversal mirrors*, Inverse Problems, 25 (2009), p. 095010.

[16] M. Fink, *Imaging of Complex Media with Acoustic and Seismic Waves*, vol. 84 of Topics in Applied Physics, Springer, 2002, ch. Acoustic Time-Reversal Mirrors, pp. 17–43.

[17] M. Fink, D. Cassereau, A. Derode, C. Prada, P. Roux, M. Tanter, J.-L. Thomas, and F. Wu, *Time-reversed acoustics*, Rep. Prog. Phys., 63 (2000), pp. 1933–1995.

[18] M. Fink and C. Prada, *Acoustic time-reversal mirrors*, Inverse Problems, 17 (2001), pp. 1761–1773.

[19] N. A. Gumerov and R. Duraiswami, *Multiple scattering from n spheres using multipole reexpansion*, J. Acoust. Soc. Amer, 112 (2002), pp. 2688–2701.

[20] C. Hazard and K. Ramdani, *Selective acoustic focusing using time-harmonic reversal mirrors*, SIAM J. Appl. Math., 64 (2004), pp. 1057–1076.

[21] S. Hou, K. Solna, and H. Zhao, *Imaging of location and geometry for extended targets using the response matrix*, J. Comput. Phys., 199 (2004), pp. 317–338.

[22] E. Iakovleva and D. Lesselier, *Multistatic response matrix of spherical scatterers and the back-propagation of singular fields*, IEEE Trans. Antenna. Prop., 56 (2008), pp. 825 – 833.

[23] A. Kirsch, *Characterization of the shape of a scattering obstacle using the spectral data of the far field operator*, Inverse Problems, 14 (1998), pp. 1489–1512.

[24] ——, *Factorization of the far-field operator for the inhomogeneous medium case and an application in inverse scattering theory*, Inverse Problems, 15 (1999), pp. 413–429.

[25] ——, *New characterizations of solutions in inverse scattering theory*, Appl. Anal., 76 (2000), pp. 319–350.

[26] ——, *The MUSIC algorithm and the factorization method in inverse scattering theory for inhomogeneous media*, Inverse Problems, 18 (2002), pp. 1025–1040.

[27] R. Kress, *Minimizing the condition number of boundary integral operators in acoustic and electromagnetic scattering*, Quart. J. Mech. Appl. Math., 38 (1985), pp. 323–341.

[28] G. Micolau, *Etude théorique et numérique de la méthode de la Décomposition de l'opérateur de Retournement Temporel (D.O.R.T.) en diffraction électromagnétique*, PhD thesis, Université d'Aix-Marseille, June 2001.

[29] B. Pinçon and K. Ramdani, *Selective focusing on small scatterers in acoustic waveguides using time reversal mirrors*, Inverse Problems, 23 (2007), pp. 1–25.

[30] C. Prada, S. Manneville, D. Spoliansky, and M. Fink, *Decomposition of the time reversal operator: detection and selective focusing on two scatterers*, J. Acoust. Soc. Am., 9 (1996), pp. 2067–2076.

[31] E. Stein, *Harmonic analysis: real-variable methods, orthogonality, and oscillatory integrals*, vol. 43 of Princeton Mathematical Series, Princeton University Press, Princeton, NJ, 1993.

[32] B. Thierry, *Analyse et Simulations Numériques du Retournement Temporel et de la Diffraction Multiple*, PhD thesis, Nancy Université, September 2011.

[33] H. Tortel, G. Micolau, and M. Saillard, *Decomposition of the time reversal operator for electromagnetic scattering*, J. Electromagn. Waves Appl., 13 (1999), pp. 687–719.

[34] R. Wong, *Asymptotic approximations of integrals*, vol. 34 of Classics in Applied Mathematics, Society for Industrial and Applied Mathematics (SIAM), Philadelphia, PA, 2001.

[35] A. Zaanen, *Linear analysis. Measure and integral, Banach and Hilbert space, linear integral equations*, Interscience Publishers Inc., New York, 1953.

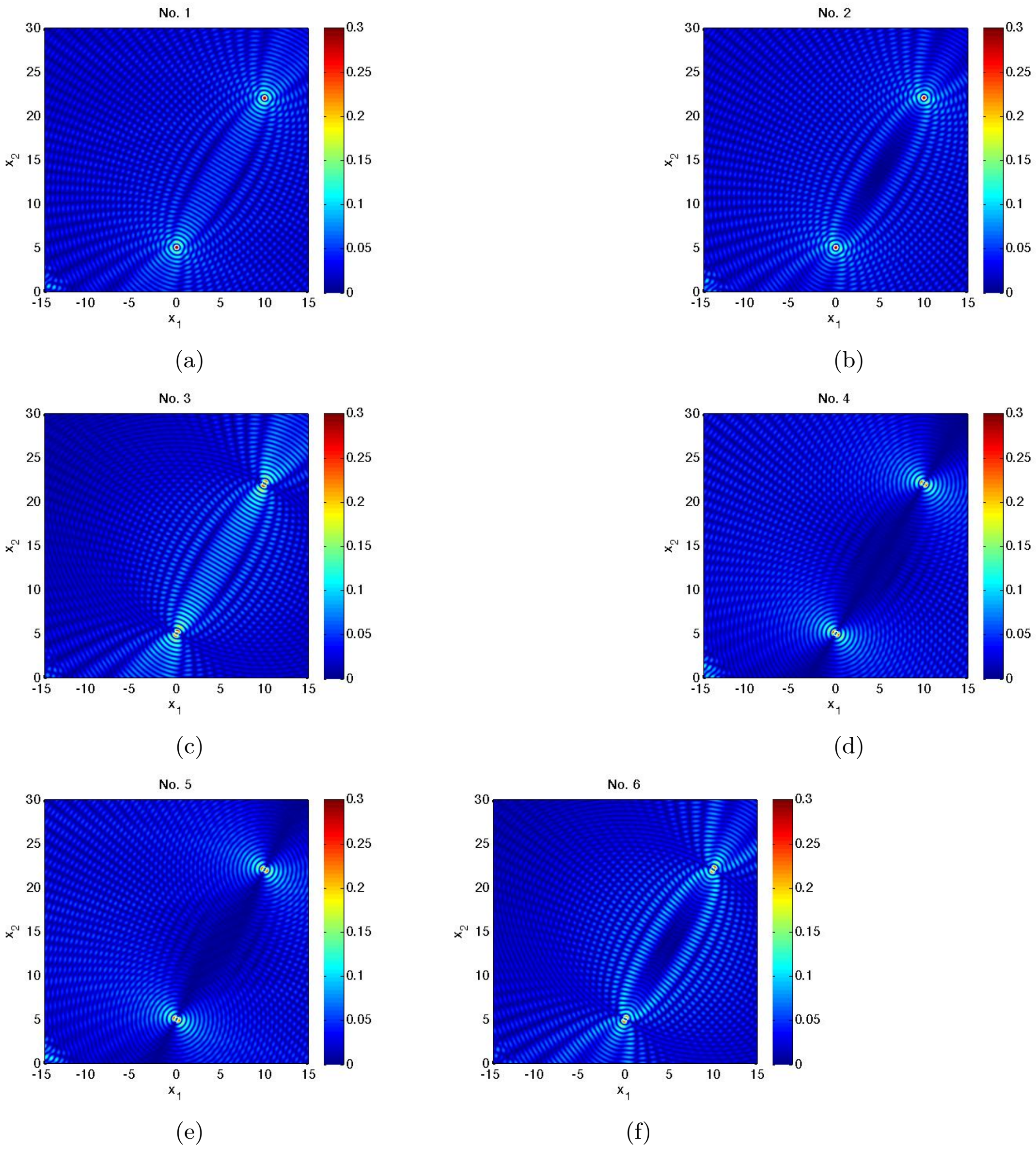

Figure 6: Two inclusions with identical magnetic and dielectric contrast (Example 2b). The Herglotz waves do selectively focus on both inclusions.

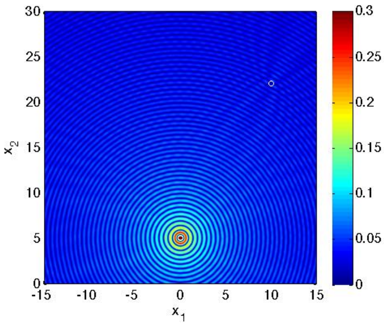

(a)

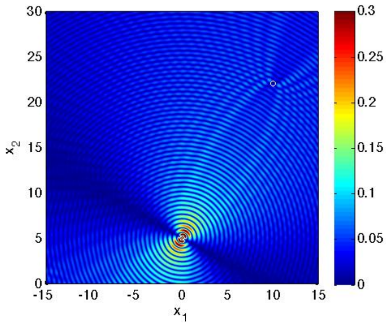

(b)

Figure 7: (a) linear combination of the first and second Herglotz waves, (b) linear combination of third and sixth Herglotz wave function of Example 2b.

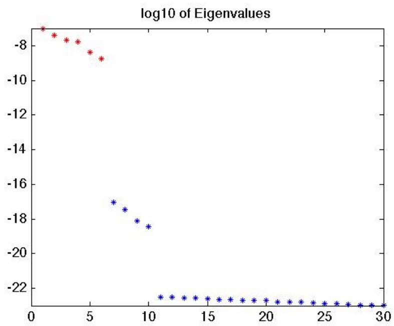

(a) No added noise

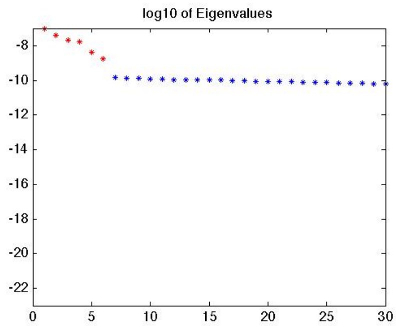

(b) 4% noise

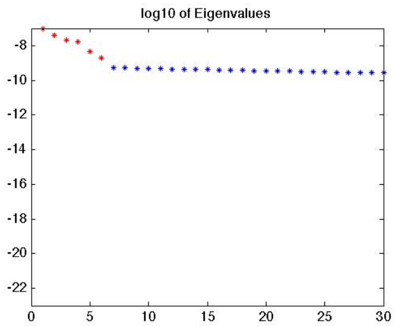

(c) 8% noise

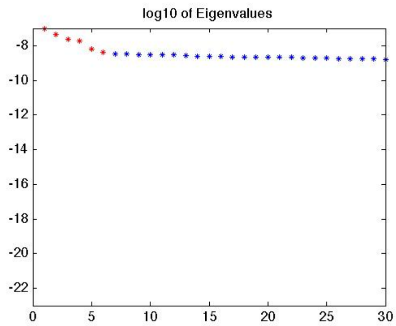

(d) 20% noise

Figure 8: We present the eigenvalues of Example 3a (using the open symmetric TRM (6.1) for different levels of noise. In (d) we observe that the first six eigenvalues are not anymore significant larger than the subsequent eigenvalues.

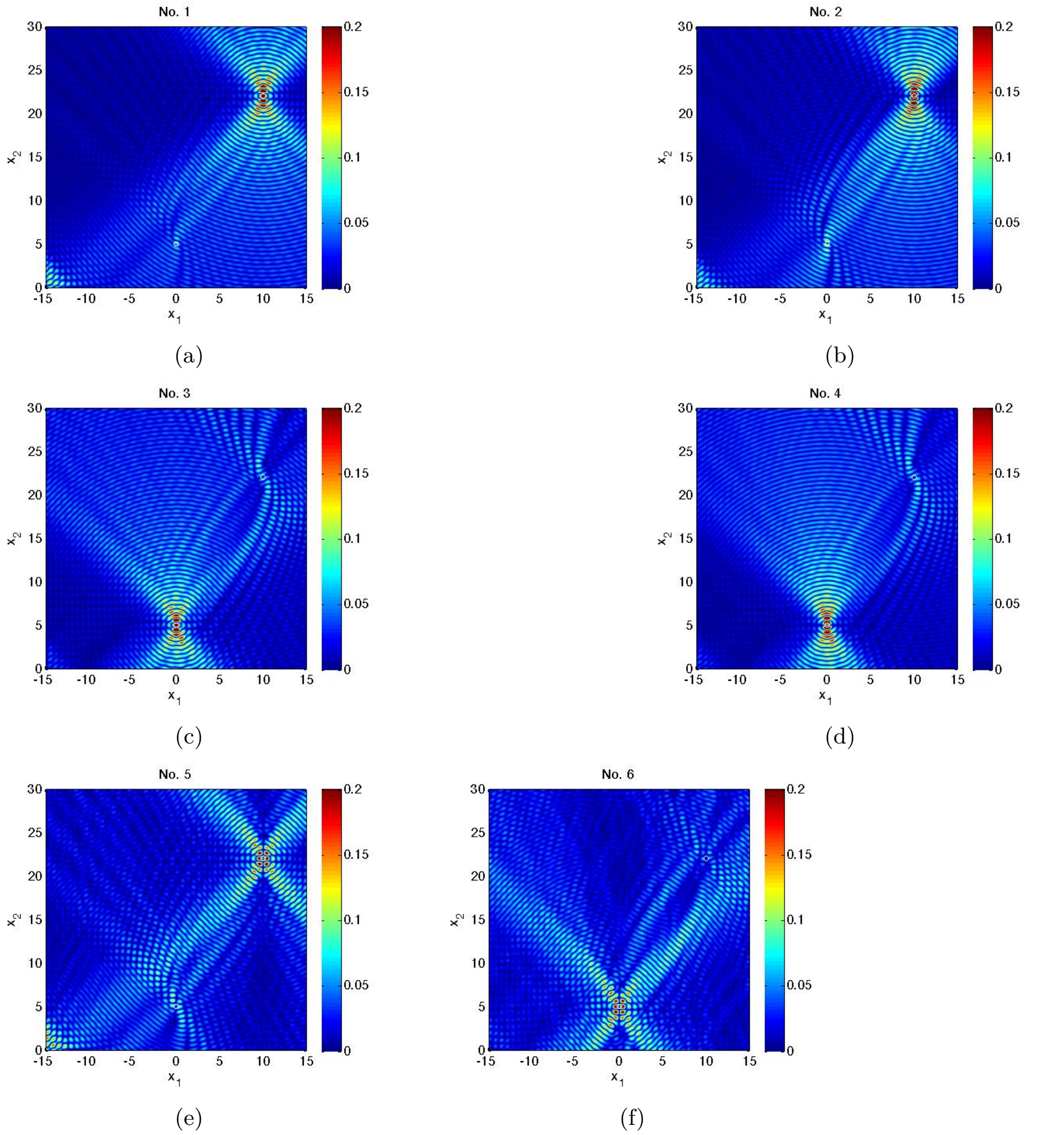

Figure 9: The DORT method for the open symmetric TRM (6.1). We show the absolute values of the Herglotz waves obtained from using the setup of Example 3a with 8% noise.

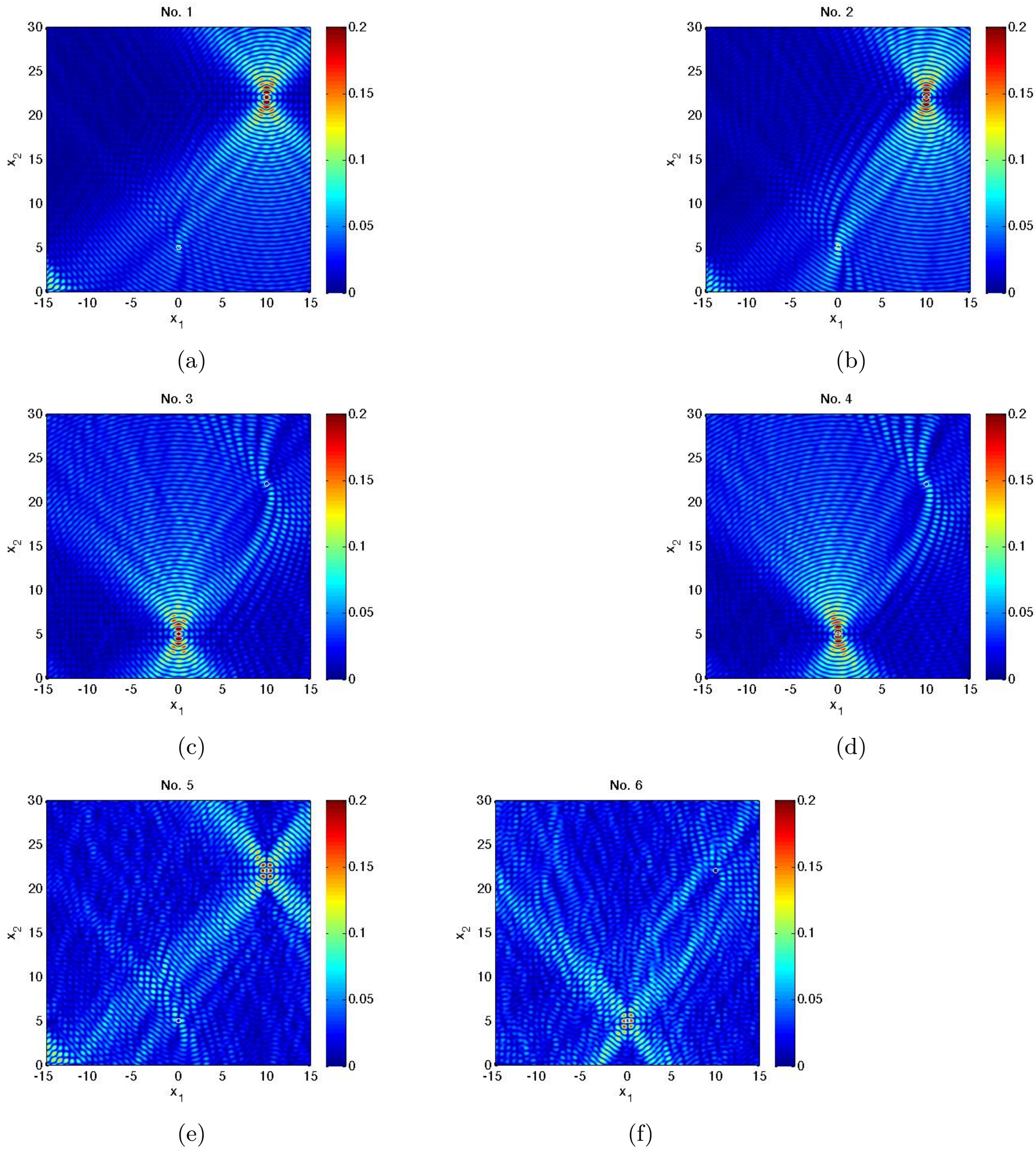

Figure 10: The DORT method for the open symmetric TRM (6.1). We show the absolute values of the Herglotz waves obtained from using the setup of Example 3a with 20% noise.

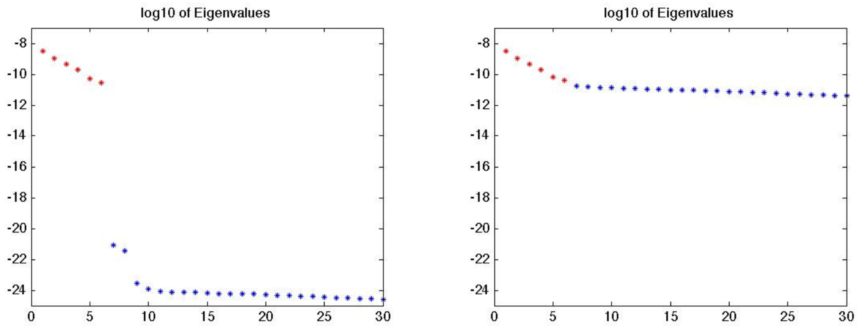

(a) No noise

(b) 8% noise

Figure 11: We present the eigenvalues for the non symmetric open TRM (6.2) without and with noise.

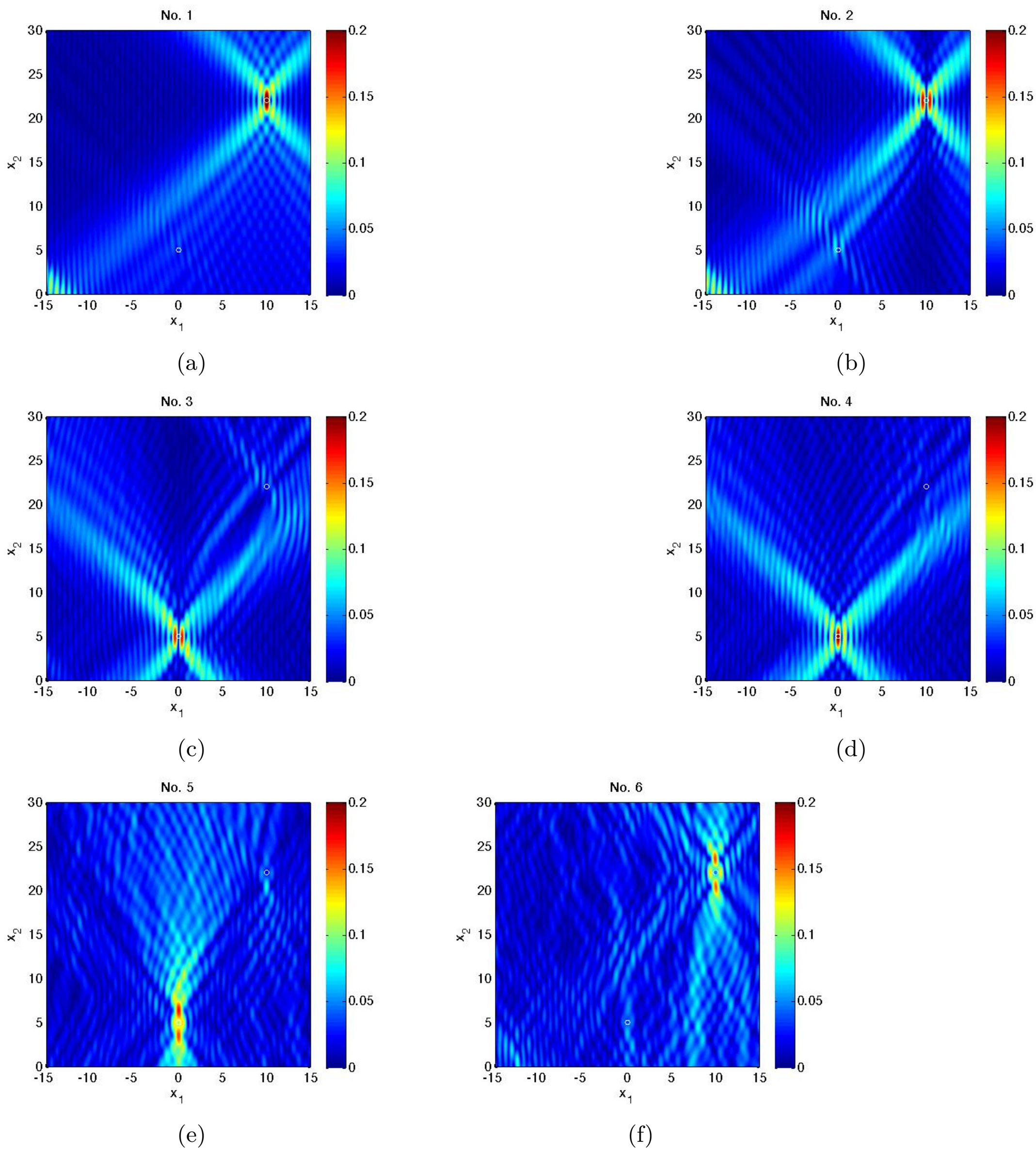

Figure 12: The absolute values of the Herglotz waves for Example 3b, using an open non symmetric TRM (6.2) with noise of 8%.